doi:10.1093/brain/awy077 BRAIN 2018: 141; 1753–1769 | 1753

BRAIN
A JOURNAL OF NEUROLOGY

Mutant LRRK2 mediates peripheral and central immune responses leading to neurodegeneration *in vivo*

Elena Kozina,[1,2] Shankar Sadasivan,[1] Yun Jiao,[1,3] Yuchen Dou,[1] Zhijun Ma,[4] Haiyan Tan,[5] Kiran Kodali,[5] Timothy Shaw,[5,6] Junmin Peng[1,3,5] and Richard J. Smeyne[1,2]

Missense mutations in the leucine rich repeat kinase 2 (*LRRK2*) gene result in late-onset Parkinson's disease. The incomplete penetrance of LRRK2 mutations in humans and LRRK2 murine models of Parkinson's disease suggests that the disease may result from a complex interplay of genetic predispositions and persistent exogenous insults. Since neuroinflammation is commonly associated with the pathogenesis of Parkinson's disease, we examine a potential role of mutant LRRK2 in regulation of the immune response and inflammatory signalling *in vivo*. Here, we show that mice overexpressing human pathogenic LRRK2 mutations, but not wild-type mice or mice overexpressing human wild-type LRRK2 exhibit long-term lipopolysaccharide-induced nigral neuronal loss. This neurodegeneration is accompanied by an exacerbated neuroinflammation in the brain. The increased immune response in the brain of mutant mice subsequently has an effect on neurons by inducing intraneuronal LRRK2 upregulation. However, the enhanced neuroinflammation is unlikely to be triggered by dysfunctional microglia or infiltrated T cells and/or monocytes, but by peripheral circulating inflammatory molecules. Analysis of cytokine kinetics and inflammatory pathways in the peripheral immune cells demonstrates that LRRK2 mutation alters type II interferon immune response, suggesting that this increased neuroinflammatory response may arise outside the central nervous system. Overall, this study suggests that peripheral immune signalling plays an unexpected—but important—role in the regulation of neurodegeneration in LRRK2-associated Parkinson's disease, and provides new targets for interfering with the onset and progression of the disease.

1 Department of Developmental Neurobiology, St. Jude Children's Research Hospital, 262 Danny Thomas Blvd, Memphis TN 38105, USA
2 Department of Neurosciences, Jefferson Hospital for Neuroscience, Thomas Jefferson University, 900 Walnut St, Philadelphia PA 19107, USA
3 Department of Structural Biology, St. Jude Children's Research Hospital, 262 Danny Thomas Blvd, Memphis TN 38105, USA
4 Department of Hematology, St. Jude Children's Research Hospital, 262 Danny Thomas Blvd, Memphis TN 38105, USA
5 St. Jude Proteomics Facility, St. Jude Children's Research Hospital, 262 Danny Thomas Blvd, Memphis TN 38105, USA
6 Department of Computational Biology, St. Jude Children's Research Hospital, 262 Danny Thomas Blvd, Memphis TN 38105, USA

Correspondence to: Richard Jay Smeyne, PhD
Department of Neuroscience
Thomas Jefferson University
400 South 9th Street
Room 444
Philadelphia, PA 19107
USA
E-mail: Richard.smeyne@jefferson.edu

Received October 23, 2017. Revised January 25, 2018. Accepted February 1, 2018. Advance Access publication March 21, 2018

Keywords: LRRK2; Parkinson's disease; inflammation; microglia; cytokines

Abbreviations: LPS = lipopolysaccharide; SNpc = substantia nigra pars compacta; WT-OX = mice overexpressing human wild-type LRRK2

Introduction

Pathogenic missense mutations in the leucine rich repeat kinase 2 (*LRRK2*) gene (formerly known as PARK8), result in an autosomal dominant late-onset Parkinson's disease with clinical and pathological phenotypes similar to idiopathic Parkinson's disease (Zimprich *et al.*, 2004). In most cases, LRRK2-associated Parkinson's disease is difficult to distinguish clinically from sporadic forms of the disease in terms of age of onset, disease progression and motor symptoms, including tremor, rigidity, postural instability and bradykinesia (Haugarvoll *et al.*, 2008; Healy *et al.*, 2008; Haugarvoll and Wszolek, 2009). In terms of pathology, both sporadic- and LRRK2-induced Parkinson's disease are characterized by the preferential loss of dopaminergic neurons in the substantia nigra pars compacta (SNpc), the presence of intracellular α-synuclein-positive inclusions (Lewy bodies) in surviving SNpc dopaminergic neurons and decreased dopamine in the striatum (Wider *et al.*, 2010).

LRRK2 is a large, complex protein containing six functional domains, two of which have known enzymatic activities; a ROC domain (GTPase activity) and a MAPKK domain (kinase activity). There are numerous single-nucleotide substitutions in each of these domains that have been shown to be pathogenic (West *et al.*, 2005, 2007), including: G2019S, R1441G/C/H, Y1699C, I2020T, N1437H, G2385R, I2020T, I2012T and R1941H (Funayama *et al.*, 2005, 2006; Khan *et al.*, 2005; Lu *et al.*, 2005; Haugarvoll and Wszolek, 2009; Satake *et al.*, 2009; Bekris *et al.*, 2010; Ross *et al.*, 2011; Puschmann *et al.*, 2012). The G2019S mutation located within the MAPKK domain is the most common cause of familial Parkinson's disease, found in up to 41% of the Parkinson's disease cases in North African Arab populations (Lesage *et al.*, 2006; Kumari and Tan, 2009), and 18% of Ashkenazi Jewish Parkinson's disease patients (Ozelius *et al.*, 2006). The second most prevalent mutation, R1441G, located in the GTPase ROC domain, is present in about 46% of familial Parkinson's disease that has an origin in the Basque region in Spain (Gaig *et al.*, 2006; Gorostidi *et al.*, 2009). In addition, LRRK2 mutations have been found in 5–10% of sporadic cases (Healy *et al.*, 2008), suggesting that the mutations are linked to a common aetiology of the disease (Kumari and Tan, 2009).

In vitro studies demonstrated that Parkinson's disease-linked mutations in the *LRRK2* gene result in increased kinase activity, which is correlated with enhanced neuronal toxicity (West *et al.*, 2005; Greggio *et al.*, 2006; Luzon-Toro *et al.*, 2007). In fact, toxic effects of mutant LRRK2 overexpression have been shown to be attenuated by pharmacological inhibition of LRRK2 kinase activity (Lee *et al.*, 2010). Additionally, kinase-dead LRRK2 was shown to be non-toxic to neurons (Greggio *et al.*, 2006; Smith *et al.*, 2006; Skibinski *et al.*, 2014). Based on these studies, it has been proposed that the pathological mechanism in LRRK2 Parkinson's disease could be driven by a gain of function that results in increased kinase activity (Greggio *et al.*, 2006). Initial *in vitro* studies using artificial substrates reported that only one mutation (G2019S) increases kinase activity, while other Parkinson's disease-associated mutations (R1441G/C/H, I2020T, Y1699C) did not appear to have any significant effect on kinase activity (Jaleel *et al.*, 2007; Nichols *et al.*, 2010). However, recent *in vivo* studies have shown that LRRK2 mutations lying outside of the MAPKK domain (i.e. R1441G) can also lead to increased autophosphorylation (Sheng *et al.*, 2012) as well as phosphorylation of a number of proteins, including those in the Rab family (West *et al.*, 2005; Steger *et al.*, 2016).

Although LRRK2 mouse models have shown impaired dopaminergic neurotransmission (Li *et al.*, 2009; Tong *et al.*, 2009), autophagic and mitochondrial abnormalities, and reduced neurite complexity (Ramonet *et al.*, 2011), the majority of studies examining LRRK2 transgenic or knock-in mice do not report any apparent histopathological changes including the selective loss of dopaminergic neurons nor motor dysfunction (Tong *et al.*, 2009; Li *et al.*, 2010; Melrose *et al.*, 2010; Herzig *et al.*, 2012; Maekawa *et al.*, 2012; Longo *et al.*, 2014). The lack of manifestation of the most important Parkinson's disease hallmarks in these murine LRRK2 models, along with the evidence from epidemiological studies of incomplete penetrance of LRRK2 mutations in Parkinson's disease patients (Bonifati, 2007; Goldwurm *et al.*, 2007; Latourelle *et al.*, 2008; Xiromerisiou *et al.*, 2012), suggest that other genetic factors or specific environmental insults might be required for mutant LRRK2 to trigger nigral cell loss (Lee and Cannon, 2015).

One of the most striking hallmarks of Parkinson's disease, observed in both sporadic and familial LRRK2 patients, is a neuroinflammation characterized by increased cytokines level in the brain and CSF, extensive microglial activation, and infiltration of peripheral immune cells into the brain's parenchyma (Rentzos *et al.*, 2007; Brodacki *et al.*, 2008; Brochard *et al.*, 2009; Dufek *et al.*, 2009; Hofmann *et al.*, 2009; Deleidi and Gasser, 2013). Several *in vitro* studies demonstrated that wild-type LRRK2 expression is induced upon IFN-γ stimulation in peripheral immune cells and in BMDMs after exposure to microbial pathogens (Gardet *et al.*, 2010; Hakimi *et al.*, 2011). Additionally, wild-type LRRK2 has been suggested to activate NF-κB signalling in HEK293T cells (Gardet *et al.*, 2010). Furthermore, LRRK2 knockout rats are partially

protected from neurodegeneration induced by α-synuclein overexpression or intranigral lipopolysaccharide (LPS) exposure, suggesting that inhibition of LRRK2 with kinase inhibitors might have a neuroprotective effect in Parkinson's disease (Daher *et al.*, 2014). However, previous studies have not examined the role of pathogenic missense LRRK2 mutations in the peripheral and/or central immune response, glial activation and their role in subsequent neuronal death. Furthermore, while a growing amount of evidence suggests that many neurodegenerative diseases have an inflammatory component, the initiating factor(s) and whether these signals arise inside or outside of the CNS are not known. Therefore, in this study we sought to determine whether LRRK2 dysfunction induces a cross-talk between the periphery and the CNS immune systems to mediate both neuroinflammation and the degeneration of dopaminergic neurons. We triggered the innate immune response in mice overexpressing the two most common pathogenic LRRK2 mutations with systemic administration of an endotoxin, LPS, and analysed the neurodegenerative processes and development of immune response in both the CNS and periphery. These studies expand previous observations made *in vitro* or in LRRK2 knockout mouse models by demonstrating that acute endotoxaemia in LRRK2 mutant mice causes long-term neuronal loss and an exacerbated immune response in the brain compared to wild-type mice. However, the accelerated neuroinflammation in mutant mice is not triggered by dysfunctional microglia or invaded T cells and/or monocytes, but is mediated by circulating inflammatory molecules that are dysregulated by mutant LRRK2.

Materials and methods

Animals and LPS administration

In this study, 2-, 3-, 12- and 24-month-old FVB/NJ, C57BL/6J, FVB/N-Tg(LRRK2*R1441G)135Cjli/J, FVB/N-Tg(LRRK2)1Cjli/J (WT-OX), B6;C3-Tg(PDGFB-LRRK2*G2019S)340Djmo/J, C57BL/6J-Tg(LRRK2*R1441G)3IMjff/J and C57BL/6J-Tg(LRRK2*G2019S)2AMjff/J (all Jackson Laboratory) mice were used. In all experiments, age- and background strain-matched littermate mice were used as wild-type controls for transgenic strains. All animals were housed within the vivarium at St. Jude Children's Research Hospital or Thomas Jefferson University and maintained on a 12:12-h light/dark cycle with *ad libitum* food and water. All of the experimental procedures in the animals were performed in accordance with the NIH Guide for the Care and Use of Laboratory Animals and all protocols, were approved by the St Jude Children's Research Hospital (Protocol 270) or Thomas Jefferson University (Protocol 1892) IACUCs. Experiments were carried out in accordance with The Code of Ethics of the World Medical Association (Declaration of Helsinki) for animal experiments.

Two- and 3-month-old mice were injected intraperitoneally with 0.9% sterile NaCl or LPS (5 mg/kg; *Escherichia coli* serotype O111:B4; 500 000 endotoxin units/mg) (Sigma-Aldrich). Warming of animals after injections was used to decrease hypothermic effects of the LPS (Romanovsky *et al.*, 1997; Paul *et al.*, 1999). All experimental procedures were performed under pathogen-free conditions.

Microglia isolation

Mouse adult microglia were isolated as described previously (Frank *et al.*, 2006; Moussaud and Draheim, 2010; Lee and Tansey, 2013). The purity and the phenotype of microglia were verified by reverse transcription-quantitative polymerase chain reaction (RT-qPCR) and western blot. For details see the online Supplementary material.

Single brain cell suspension preparation and FACS

Mouse adult brain tissue was dissociated for fluorescence-activated cell sorting (FACS) following the modified protocol of Brewer (Brewer and Torricelli, 2007). Samples were sorted for $Thy^+/CD3^-$, $O4^+$ and $GLAST^+$ (Schwarz *et al.*, 2013; Sharma *et al.*, 2015) using a FACSAria cell sorter (BD Biosciences). The purity of sorted cells was verified by western blot. For more details, see the online Supplementary material.

Peripheral blood mononuclear cell separation

Blood was collected from the heart of deeply anaesthetized mice into 10% EDTA-treated vacuum tubes, mixed 1:1 with sterile PBS and separated in lymphocytes separation medium (Corning). Samples were centrifuged for 30 min at 400*g* at room temperature and then the leucocyte 'white' layer was carefully aspirated and placed into sterile tubes. Cells were washed twice with three volumes of sterile PBS, centrifuged for 10 min at 200*g* at room temperature, and then stored at −80°C until assayed. For tandem mass tagging (TMT)-based proteomics experiments, leucocytes for each genotype and treatment were pooled from three to six mice.

Flow cytometry and FACS

For flow cytometric analysis, blood was collected from the heart of deeply anaesthetized mice into 10% EDTA-treated vacuum tubes. After red blood cell lysis with ammonium chloride solution, peripheral blood mononuclear cells (PBMCs) were stained with antibodies against CD4 (PerCP-Cy5.5), CD8 (PE-Cy7), CD19 (APC-Cy7), CD25 (APC), CD49 (PE), Mac-1 (Alexa700), Gr-1 (PerCP) (all from BD Biosciences), B220 (eFluor605; eBiosciences), and DAPI (Molecular Probes) for 30 min at 4°C. Data were acquired using a FACSCalibur flow cytometer (BD Biosciences) and analysed with CellQuest Pro software. For FACS, blood was pooled from 15 mice into 10% EDTA-treated vacuum tubes, and then the red blood cell-depleted PBMCs were incubated with anti-CD4 (APC), anti-CD8 (PerCP-Cy5.5), anti-CD11b (Alexa 700), anti-CD14 (PE), anti-CD19 (APC-Cy7) (all antibodies from BD Biosciences) and DAPI (Molecular Probes). Sorting of defined subpopulations was performed using a FACSAria cell sorter (BD Biosciences). For details see the online Supplementary material.

Cytokine assay

Cytokine expression in serum and brain samples was analysed with the Milliplex Map Kit, MCYTOMAG-70K (Millipore) and Luminex 200™. Data were analysed using BioPlex Manager 4.1 software. For details see the online Supplementary material.

Western blot

The following antibodies were used in this study: rabbit anti-LRRK2 (1:1000; clone 41-2, Abcam by MJFF), rabbit anti-pS935 LRRK2 (1:1000; Abcam by MJFF), rabbit anti-CD11b (1:1000; Abcam), rabbit anti-NeuN (1:1000; Abcam), mouse anti-GFAP (1:1000; Sigma-Aldrich), rabbit anti-MAP2 (1:500; Cell Signaling), mouse anti-GFAP (1:500; Cell Signaling), rabbit anti-MBP (1:500; Cell Signaling), rabbit or mouse anti-β-actin (1:2000; Abcam). For detailed description of the western blot protocol see the online Supplementary material.

RT-qPCR

Microglia, leucocytes and brain samples were processed to obtain RNA in accordance with the protocol outlined in PureLink® RNA Mini Kit or ARCTURUS® PicoPure® RNA isolation Kit (Thermo Fisher Scientific). Reaction was performed using TaqMan Gene Expression Master Mix or TaqMan® Fast Advanced Master Mix in a 7300 Real Time PCR System or 7500 Fast Real Time PCR System (Applied Biosystems), respectively. All samples were run in triplicate. For detailed description see the online Supplementary material.

Quantitative analysis of proteome by 10-plex TMT-LC/LC-MS/MS

Proteomic analysis was performed as detailed in Tan *et al.* (2017). The mass spectrometry proteomics data have been deposited to the ProteomeXchange Consortium via the PRIDE [1] partner repository with the dataset identifier PXD006290 and PXD006289. For a detailed description see the online Supplementary material.

Immunohistochemistry

Immunostaining was performed as detailed in Jang et al. (2009), using antibodies directed against TH (mouse monoclonal, Sigma-Aldrich), Iba-1 (rabbit polyclonal, Wako; or goat polyclonal, Abcam), CD3 (Santa Cruz Biotechnology), Tmem119 (rabbit monoclonal; clone 28-3; provided by Prof. Ben Barres), and CCR2 (goat polyclonal, Thermo Fisher Scientific).

Stereological analysis

Stereological analysis of SNpc dopaminergic neurons and microglia were performed as detailed in Baquet *et al.* (2009).

Statistical analysis

All data are represented as mean ± standard error of the mean (SEM). Statistical analysis was performed using the GraphPad Prism® version 4.03 software. Differences between groups were determined by one-way ANOVA. If overall statistical significance was found, Tukey's *post hoc* comparisons were performed.

Results

Characterization of LRRK2 mice

Since LRRK2 mutations result in late-onset Parkinson's disease in humans (Zimprich *et al.*, 2004), we first asked whether 2-year-old transgenic mice overexpressing Parkinson's disease-linked LRRK2 mutations develop neuronal loss in the SNpc. We analysed two commercially-available transgenic strains overexpressing mutant human R1441G LRRK2 [FVB/N-Tg(LRRK2*R1441G)135Cjli/J and C57BL/6J-Tg(LRRK2*R1441G)3IMjff/J]; and two transgenic strains overexpressing mutant human G2019S LRRK2 [B6;C3-Tg(PDGFB-LRRK2*G2019S)340Djmo/J and C57BL/6J-Tg(LRRK2*G2019S)2AMjff/J]. Both strains overexpressing the human R1441G mutation were found to have the *LRRK2* transgene inserted into mChr1, while the G2019S (340Djmo/J) and G2019S (2AMjff/J) strains have human *LRRK2* transgene insertion sites in mChr3 and mChr2, respectively (Supplementary Fig. 1A). All strains analysed overexpress human mutant LRRK2 in the peripheral tissues and brain, including substantia nigra, striatum and cortex (Supplementary Fig. 1B). However, regardless of the strain background or the promoter used to drive mutant LRRK2, none of these four transgenic strains exhibited a loss of TH neurons in the SNpc or evidence of microgliosis at 2 years of age (Supplementary Fig. 1C and D). Two transgenic strains, R1441G (135Cjli/J) and G2019S (340Djmo/J), were used for the subsequent experiments (Supplementary Fig. 1E) since these have been previously characterized (Li *et al.*, 2009; Ramonet *et al.*, 2011; Mandemakers *et al.*, 2012; Bichler *et al.*, 2013; Sanchez *et al.*, 2014; Mikhail *et al.*, 2015).

Systemic inflammation induces dopaminergic-neuron loss in the substantia nigra pars compacta of mutant LRRK2 mice

Since transgenic mice overexpressing pathogenic LRRK2 mutations failed to develop an overt neurodegenerative phenotype—up to 2 years of age—we hypothesized that mutant LRRK2, acting as a stress-responsive kinase (Gardet *et al.*, 2010; Hakimi *et al.*, 2011; Lewis and Manzoni, 2012; Moehle *et al.*, 2012), would be capable of facilitating neuronal loss only under specific conditions. Thus, we addressed a potential role for mutant LRRK2 in inflammation-induced neurodegeneration by evaluating the responses of mutant LRRK2 mice and their age-and strain-matched littermate wild-type controls to the administration

of LPS (Supplementary Fig. 2A and B). To determine if LPS induces cell loss, we performed a stereological analysis of SNpc dopaminergic neurons (Baquet *et al.*, 2009) from NaCl- and LPS-treated R1441G and strain-matched wild-type littermate controls 24 h, 7 days, 2 and 7 months post-LPS. We found that 24 h after LPS there was a small but significant loss of TH-positive neurons in the SNpc of R1441G mice while no change was observed in wild-type mice. At 7 days post-LPS, the loss of SNpc TH-positive neurons progressed, after which this loss stabilized (Fig. 1A and C). Nissl staining confirmed the loss of dopaminergic neurons in the SNpc of R1441G mice 7 months post-LPS (data not shown).

To determine whether inflammation-induced neuronal loss is mutation specific, we exposed transgenic mice overexpressing mutant G2019S LRRK2 to LPS. Twenty-four hours after LPS, we found a significant loss of SNpc TH-positive dopaminergic neurons in the G2019S mice. The loss increased by 7 days after which the lesion became stable (Supplementary Fig. 2C and D). The loss of SNpc dopaminergic neurons was selective, as we observed no loss of glutamatergic pyramidal cells in the CA1 region of the hippocampus (NaCl: 39410 ± 618.5; LPS 7 months: 41867 ± 2063, $n = 3$; $P = 0.31$). Next, since both forms of mutant LRRK2 increased sensitivity of SNpc dopaminergic neurons to LPS, we examined if this effect was due to overexpression of LRRK2 itself or was specific to the mutant forms of the protein. When LPS was administered to mice overexpressing human wild-type LRRK2 (WT-OX) (Supplementary Fig. 2E and F), we observed no differences in the LPS-induced inflammatory response between wild-type and WT-OX (Supplementary Fig. 2G) or SNpc dopaminergic neuron loss (Supplementary Fig. 2H), suggesting that the neuron loss induced by LPS was dependent on mutant LRRK2.

Dopaminergic neuron loss in LRRK2 mice is not associated with the recruitment of peripheral immune cells into the brain parenchyma

Since recent studies have implicated the role of infiltrated peripheral immune cells, particularly T cells, in neuronal cell death (McGeer *et al.*, 1988; Brochard *et al.*, 2009; Cebrian *et al.*, 2014), we next examined whether the loss of dopaminergic neurons seen in LPS-treated R1441G mice is mediated through invaded T cells. Here, coronal sections

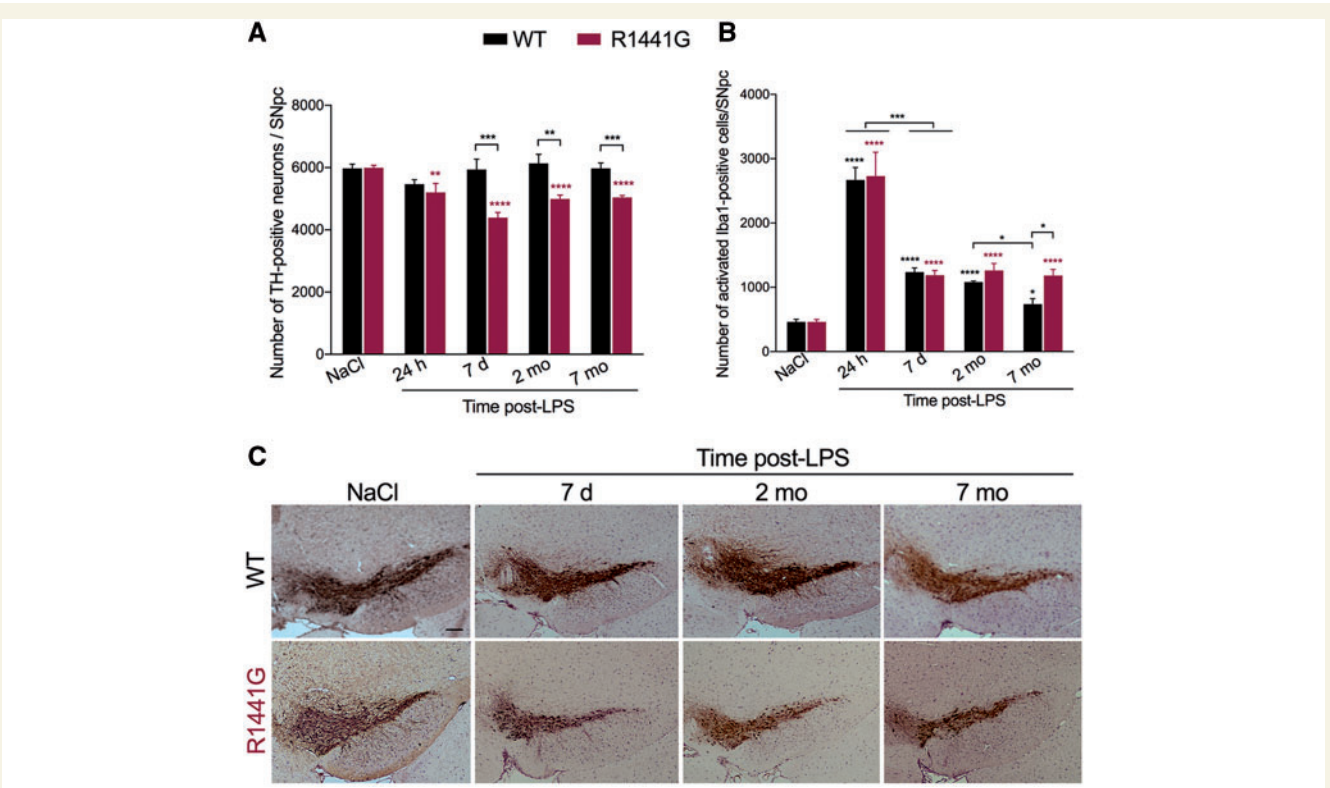

Figure 1 Systemic inflammation causes neuronal loss in the SNpc of mutant R1441G mice but not wild-type. (**A**) Loss of TH-positive dopaminergic neurons in the SNpc of R1441G mice up to 7 months (mo) after systemic LPS injection. Data are mean ± SEM, $n = 16$ for NaCl group, $n = 3$–5 for each post-LPS group. $^{**}P < 0.005$, $^{***}P < 0.001$, $^{****}P < 0.0001$. (**B**) Number of activated Iba1-positive microglial cells in the SNpc of R1441G mice and background matched non-transgenic littermates (WT) following systemic LPS injection. Data are mean ± SEM, $n = 15$ for NaCl group, $n = 3$–5 for each post-LPS group. $^{*}P < 0.05$, $^{***}P < 0.001$, $^{****}P < 0.0001$. (**C**) Representative images of TH-positive dopaminergic neurons in the SNpc of wild-type and R1441G mice 7 days (d), 2 and 7 months after LPS injection. Sections are matched at the same level of the substantia nigra (Bregma −3.08–3.16 mm) (Paxinos and Franklin, 2001). Scale bar = 100 μm.

spanning the rostral-caudal extent of the brain were immunostained for a T cell marker, CD3. However, we found no evidence for T cell infiltration either in the substantia nigra or any other brain region of R1441G mice 24 h to 7 months post-LPS (Supplementary Fig. 3A). Immunohistochemical data were further confirmed by flow cytometric analysis of a single-cell brain suspension showing no CD3-positive cells in the LPS-treated R1441G brains (Supplementary Fig. 3B). Furthermore, immunostaining against a chemokine receptor, CCR2, which is known to be expressed on peripheral monocytes and macrophages but not in brain microglia (Mildner *et al.*, 2007; Mizutani *et al.*, 2012; Chiu *et al.*, 2013), showed the lack of monocytes trafficking from the periphery (Fig. 2A). However, there was a significant increase in the number of activated Iba1-positive microglial cells in the SNpc following LPS injection with the number of Iba1 cells being higher in R1441G mice compared to wild-type mice 7 months post-LPS (Fig. 1B). Immunostaining with monoclonal antibodies that recognizes the microglia-specific transmembrane protein 119 (Tmem119) (Butovsky *et al.*, 2014; Bennett *et al.*, 2016) revealed that Tmem119 is co-localized with Iba1 following LPS treatment (Fig. 2B), suggesting that LPS-induced increase in the number of Iba1-positive cells resulted from a shift of microglial cells from a resting to an activated state rather than inducing infiltration of peripheral macrophages into the CNS.

Brain inflammatory profile is altered by mutant LRRK2

We investigated whether mutant LRRK2 alters the neuroinflammatory profile of the brain further. Thus, we assessed time-dependent changes in pro-apoptotic (TNF-α, IFN-γ, IL-1α), pro-inflammatory (IL-6) and anti-inflammatory cytokines (IL-10) as well as chemokines (CXCL-1, CXCL-10, CCL-2 (MCP-1), CCL-3 (MIP-1α) in the substantia nigra and striatum of normal and LPS-treated R1441G mice and their wild-type strain-matched littermate controls. At baseline, no significant differences in cytokine levels were observed between R1441G mice and their strain-matched littermate wild-type controls, except for small increases in CCL-2 and IFN-γ in the substantia nigra and a slight decrease in the levels of IL-10 and IL-1α in the striatum (Fig. 3A and B). However, following administration of LPS, significant differences were detected in the induction of IL-1α, IFN-γ, CXCL-1 and CXCL-10 in the substantia nigra and striatum of R1441G mice compared to wild-type controls, suggesting a generalized effect of mutant LRRK2 on the brain neuroinflammatory profile (Fig. 3C and D). Importantly, we found that IL-1α and IFN-γ, which have consistently been associated with neurodegeneration *in vivo* (Allan and Rothwell, 2001; Nesic *et al.*, 2001; Allan *et al.*, 2005; Mizuno *et al.*, 2008; Pott Godoy *et al.*, 2008; Chakrabarty *et al.*, 2011; Mangano *et al.*, 2012), remain elevated in the substantia nigra of R1441G mice even 2 months post-LPS compared to wild-type controls (Fig. 3C). To get a more detailed characterization of the altered neuroinflammatory reaction in the brain of LRRK2 mice, we performed mass spectrometry analysis (TMT) of brain tissue obtained from NaCl- and LPS-challenged wild-type (WT + LPS) and R1441G mutant mice (R1441G + LPS) (Fig. 4A). Mass spectrometry identified 10 743 proteins (< 1% false discovery rate, FDR). For LPS-treated samples, differential expression analysis between R1441G + LPS and WT + LPS found 24 upregulated and 11 downregulated proteins that satisfied the power-based $\log_2(FC) \geqslant 0.37$ and $P \leqslant 0.01$ cut-off (Fig. 4B); and 137 upregulated and 73 downregulated proteins that satisfied the $\log_2(FC) \geqslant 0.22$ and $P \leqslant 0.01$ cut-off (Supplementary Table 1). None of the genes encoding the most enriched proteins in the R1441G group are located in the region of the transgene insertion on mChr1, suggesting that the transgene insertion itself is not a direct cause of the proteomic differences. Gene set enrichment analysis revealed several pathways that are preferentially enriched in the R1441G + LPS group compared to WT + LPS, including INF-γ response, IL6-JAK-STAT3 signalling, inflammatory response and TNF-α signalling (Fig. 4C and D). We next validated the expression of selected genes that encode proteins enriched in R1441G + LPS group in an independent experiment with a higher number of replicates and found that differences in mRNA expression for most genes in the R1441G + LPS group versus the WT + LPS group were similar to the one we observed for proteins in the proteomics experiment (Fig. 4E).

Exacerbated neuroinflammatory signalling in the brain of LRRK2 mice is not directly mediated through microglia

Given that microglial cells are the primary cells in the CNS capable of responding to the inflammatory stimulus, we next hypothesized that increased neuroinflammatory signalling and subsequent neuron damage in the SNpc of R1441G mice could be mediated through activated mutant microglial LRRK2. To test this hypothesis, we used well-described methods to isolate microglial cells from the brain (Cardona *et al.*, 2006; Frank *et al.*, 2006; Moussaud and Draheim, 2010), and then analysed LRRK2 expression and/or activation following the induction of systemic inflammation. RT-qPCR of isolated microglia confirmed the high purity of isolated cells (Fig. 5A). Furthermore, acutely isolated adult microglia from different brain regions expressed significantly elevated levels of pro-inflammatory markers upon *in vivo* activation with LPS compared to microglia from NaCl-treated mice (Fig. 5B), suggesting that isolated microglia can be used to reflect the LPS-induced inflammation-associated changes seen *in vivo*. However, subsequent western blot analysis of isolated microglia showed no LRRK2 expression or LPS-induced LRRK2 upregulation (Fig. 5C). These immunoblot data

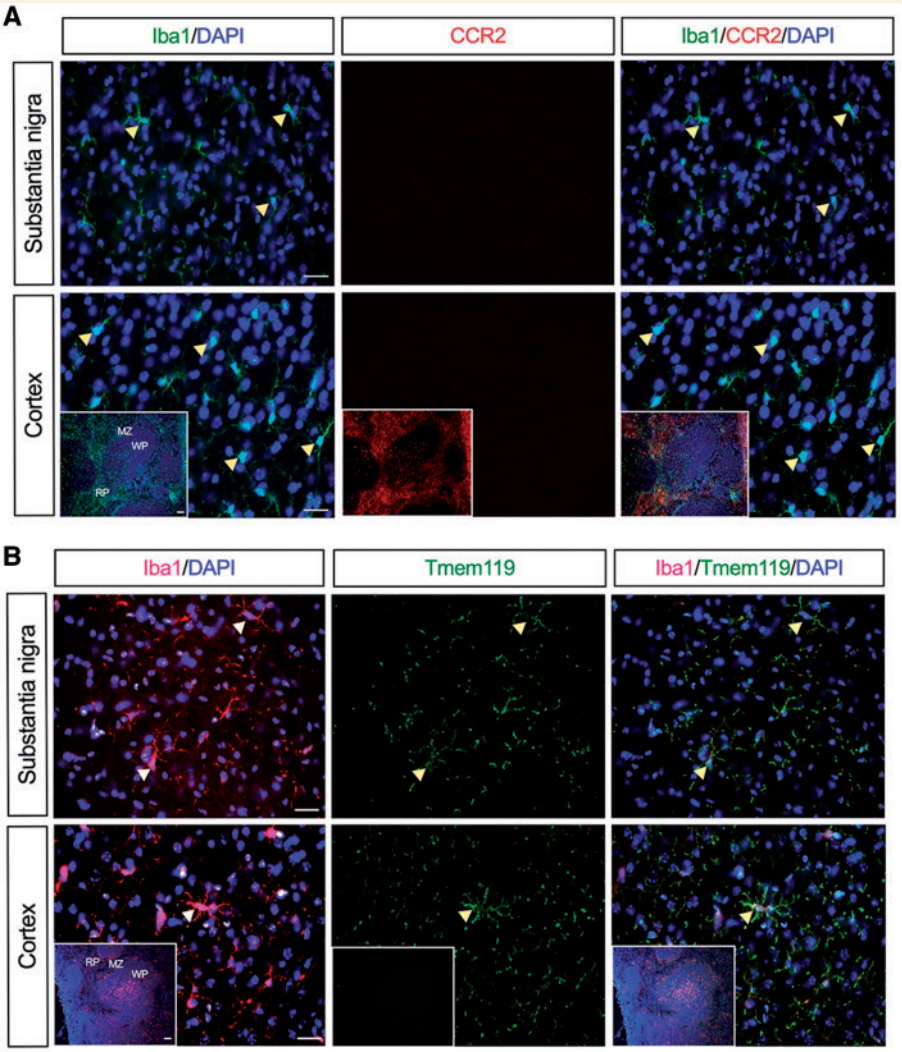

Figure 2 Lack of monocytes trafficking from the periphery into the brain of LPS-treated R1441G mice. (**A**) No CCR2 expression was seen in the substantia nigra and cortex of R1441G mice 24 h post-LPS. (**B**) Microglia-specific marker, Tmem119, is co-expressed in Iba1-positive microglia in the substantia nigra and cortex of R1441G mice 24 h post-LPS. *Insets* show spleen sections that were used as a positive and negative control for CCR2 and Tmem119 staining, respectively. Scale bar = 50 μm. Scale bar in *insets* = 100 μm. MZ = marginal zone; RP = red pulp; WP = white pulp.

were confirmed by RT-qPCR showing almost no detectable *Lrrk2* mRNA expression in microglia isolated from the midbrain of R1441G mice compared to the substantia nigra tissue (Fig. 5D). We also found no pS935 expression in isolated microglia (data not shown). Unexpectedly, these data for the first time suggest that 'mutant' microglia do not directly alter neuroinflammation in the brain of mice overexpressing pathogenic LRRK2. However, although not seen in the brain microglia, a significant and prolonged mutant LRRK2 upregulation (normal and phosphorylated) was found in the substantia nigra (Fig. 5E–G) and the whole brain tissue (Fig. 5H) of LPS-treated R1441G mice compared to LPS-treated strain-matched wild-type littermate controls. To determine what cells were responsible for the observed mutant LRRK2 upregulation, we used a FACS protocol (Brewer and Torricelli, 2007; Guez-Barber *et al.*, 2012; Schwarz *et al.*, 2013; Sharma *et al.*, 2015) to purify neurons, astrocytes and oligodendrocytes from the adult mouse brain after *in vivo* stimulation with LPS (Supplementary Fig. 4A and B). Sorted cells were consistently >95% viable based on DAPI staining (Supplementary Fig. 4C). We confirmed the identity and purity of each sorted population ($Thy1^+/CD3^-$ neurons, $GLAST^+$ astrocytes, $O4^+$ oligodendrocytes) using known cell type-specific proteins (Supplementary Fig. 4D). Further examination of sorted cell populations revealed that LRRK2 was highly expressed in the sorted $Thy1^+/CD3^-$ neurons (Fig. 5I), and upregulated in neurons following LPS administration, but not in astrocytes or oligodendrocytes (Fig. 5J). Taken together, these data clearly suggest that ongoing inflammation has a long-term effect on intraneuronal mutant LRRK2 expression *in vivo*.

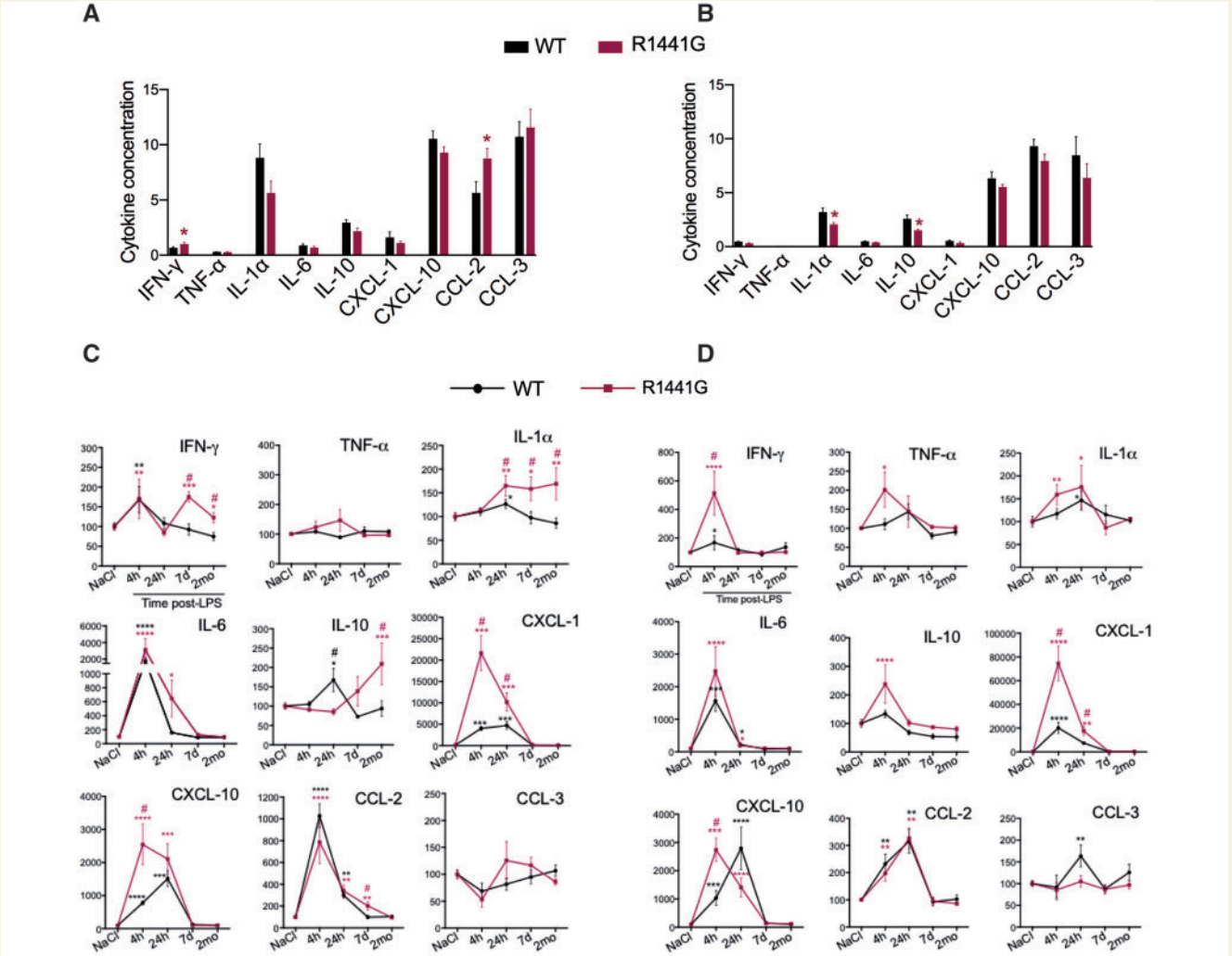

Figure 3 Mutant LRRK2 accelerates LPS-induced cytokine upregulation in the brain. (**A** and **B**) Cytokine profile of the substantia nigra (**A**) and striatum (**B**) of NaCl-injected R1441G mice and wild-type littermate controls. Data are expressed as pg/mg total protein. Data are mean ± SEM, $n = 22–23$. *$P < 0.05$ versus wild-type littermate controls. (**C** and **D**) Cytokines profile of the substantia nigra (**C**) and striatum (**D**) of R1441G mice and wild-type littermate controls at different time-points after LPS injection. Data are mean ± SEM, $n = 15–16$ for 24 h post-LPS, $n = 5–8$ for 4 h, 7 days, 2 months post-LPS. *$P < 0.05$, **$P < 0.005$, ***$P < 0.001$, ****$P < 0.0001$ versus NaCl group; $^{\#}P < 0.05$ versus LPS-treated wild-type. For each genotype, data in LPS-treated groups are expressed as the percentage of NaCl control.

LPS-induced peripheral cytokines secretion and activation of immune pathways in leucocytes are exacerbated by mutant LRRK2

Based on the above experiments showing no LRRK2 expression and/or activation in brain microglia along with the evidence for lack of myeloid and T cell infiltration, we postulated that increased neuroinflammation in the brain of mutant mice could be mediated through circulating inflammatory mediators, and that the neurotoxic signals in mice carrying LRRK2 mutations might be generated outside the CNS. To test this hypothesis, we measured the protein level of peripherally-produced cytokines in the serum of wild-type and R1441G mice in response to LPS (Fig. 6A). First, we found that NaCl-injected wild-type or R1441G mice showed no genotype-related differences in cytokine concentration (Fig. 6B). However, following LPS administration, the expression wave of serum cytokines differed significantly starting 4 h after LPS; with increased levels of IFN-γ, IL-6, IL-10, CCL-5, G-CSF and M-CSF measured in R1441G mice compared to wild-type mice (Fig. 6C). To determine whether elevated cytokines affect LRRK2 expression in the peripheral immune cells, we isolated leucocytes from R1441G and wild-type littermate controls, and found that mutant LRRK2 upregulation was ~10-fold greater in LPS-treated R1441G leucocytes than that in wild-type cells (Fig. 6D). We next carried out flow cytometric analysis (Supplementary Fig. 5A and B) to characterize peripheral

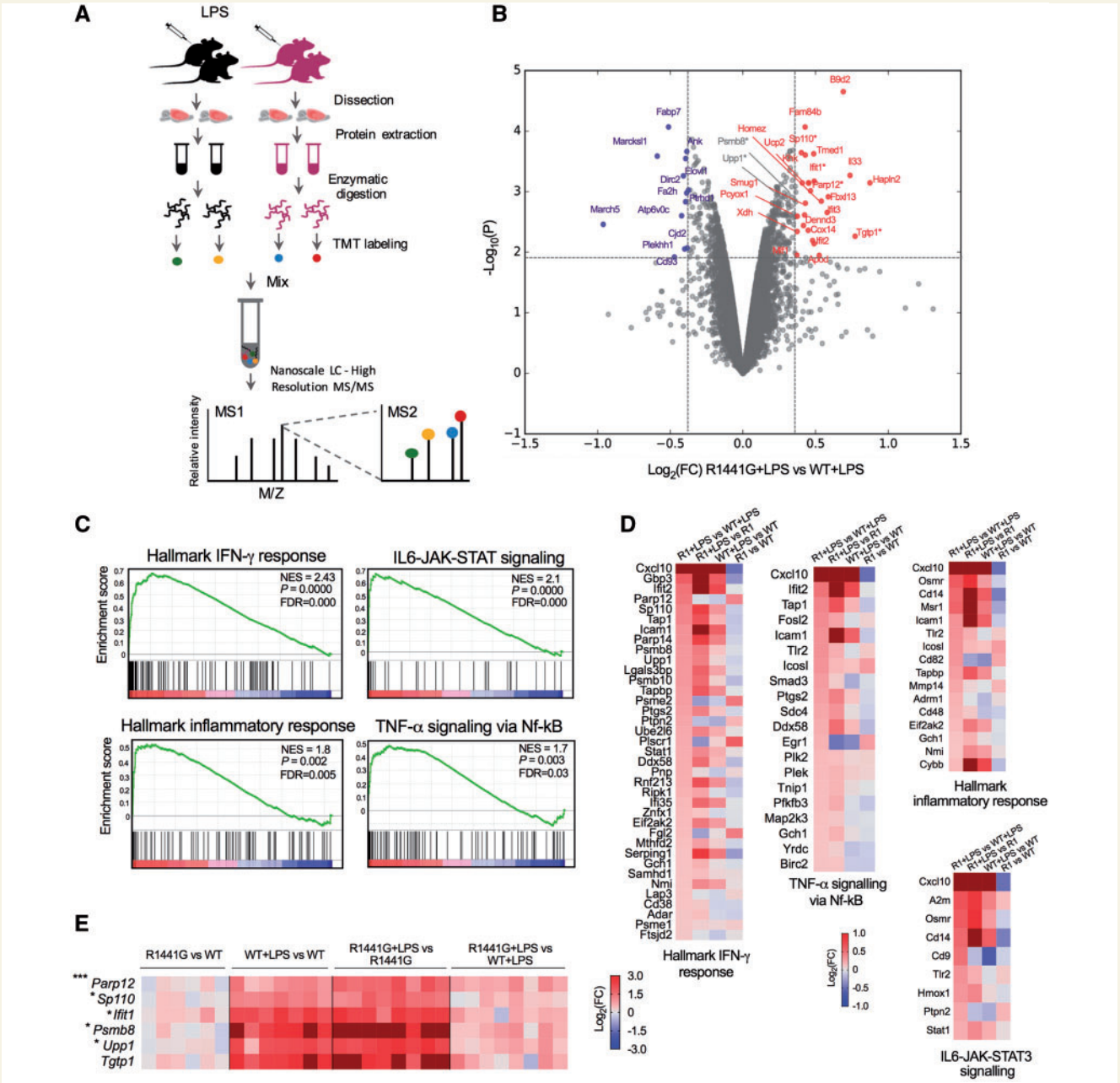

Figure 4 Brain inflammatory profile is altered by mutant LRRK2. (**A**) Experimental scheme for proteomic analysis of the brain samples. (**B**) Volcano plots of proteomic data from the brain of LPS-treated R1441G and wild-type littermate control mice. Log_2fold-change(FC) is plotted across the *x*-axis and *P*-value is plotted on the *y*-axis. The red and blue nodes represent proteins upregulated and downregulated, respectively, in the R1441G + LPS group that satisfy $\log_2(FC) \geqslant 0.37$ and $P \leqslant 0.01$ cut-off. All differentially expressed proteins in the brain of LPS-treated wild-type and R1441G mice determined by quantitative proteomics analysis are listed in Supplementary Table 1. (**C**) GSEA plots and (**D**) heat maps showing upregulation of proteins involved in inflammatory response pathways in the brain of R1441G mice by comparison with littermate wild-type mice following *in vivo* LPS administration. Each bar at the bottom of the panel represents a member protein of the respective pathway. For each gene set enrichment assay, the nominal *P*-value, normalized enrichment score (NES) and FDR are shown. (**E**) Heat map showing mRNA expression of the selected genes in the brain of NaCl- and LPS-treated R1441G and wild-type littermate mice validated in an independent experiment. Target gene expression level was normalized to β-actin. Data are mean ± SEM, $n = 6$ for NaCl group; $n = 7$–8 for LPS group. $^*P < 0.05$, $^{***}P < 0.001$, R1441G + LPS versus WT + LPS. Proteins encoded by validated genes and satisfy $\log_2(FC) \geqslant 0.37$ cut-off are labelled with red asterisks in **B**. Other proteins encoded by validated genes are labelled with grey asterisks in **B**.

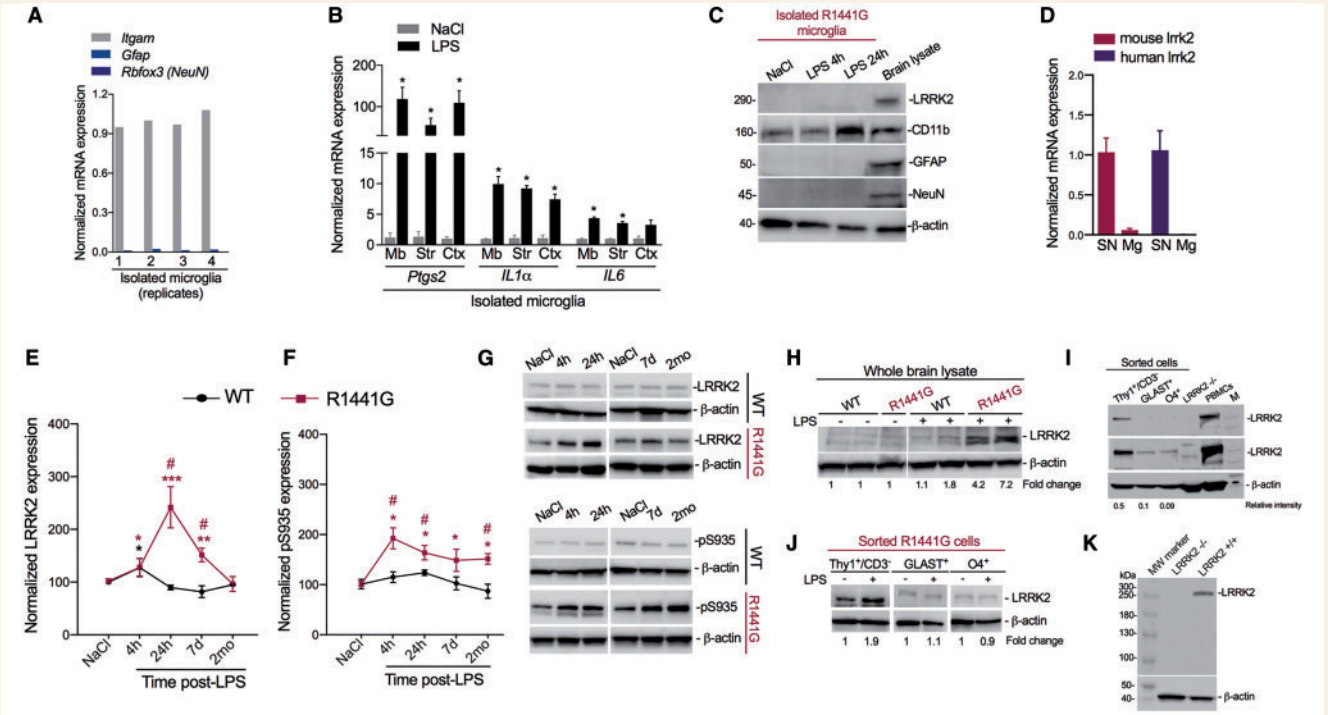

Figure 5 Exacerbated neuroinflammation in the brain of LRRK2 mice is not mediated through microglia. (**A**) Normalized expression of *Itgam*, *Gfap* and *Rbfox3* (*NeuN*) mRNA in isolated adult microglia from four different independent experiments was used to confirm the purity of isolated microglia. (**B**) Induction of inflammatory genes expression in acutely isolated adult microglia following *in vivo* LPS administration [$n = 2$; midbrain (Mb), striatum (Str) and cortex (Ctx) were pooled from three mice]. Inflammatory genes expression was normalized to the β-actin mRNA. Data are mean ± SEM. $^*P < 0.05$ versus NaCl group. (**C**) Immunoblot of protein isolated from microglia obtained from NaCl- and LPS-treated R1441G mice. CD11b, GFAP and NeuN expression was used to confirm the purity of isolated microglia. (**D**) Normalized expression of mouse and human *Lrrk2* mRNA in the substantia nigra and isolated midbrain microglia (Mg) from the brain of R1441G mice. Data are mean ± SEM; $n = 3$–6 (midbrain microglial cells were pooled from three R1441G mice, each pooled sample: $n = 1$). *Lrrk2* mRNA expression levels were normalized to β-actin. (**E**–**G**) Total and pS935 LRRK2 upregulation in the substantia nigra following single LPS administration. Data are mean ± SEM; $n = 19$–20 for NaCl group, $n = 5$ for 4 h post-LPS, $n = 9$–11 for 24 h post-LPS, $n = 6$–10 for 7 days post-LPS, $n = 4$–5 for 2 months post-LPS; $^*P < 0.05$, $^{**}P < 0.001$, $^{***}P < 0.0001$. Total and pS935 LRRK2 protein levels were normalized to the level of β-actin. (**H**) Total LRRK2 upregulation in the whole brain tissue of R1441G mice 24 h following single LPS administration. (**I**) LRRK2 expression in sorted neurons ($Thy1^+/CD3^-$), astrocytes ($GLAST^+$) and oligodendrocytes ($O4^+$). *Top* two panels are different exposures of the same western blot. Relative band intensities of LRRK2 in each cell population were normalized to β-actin. $Lrrk2^{-/-}$ cortex sample was included as a negative control. (**J**) LRRK2 expression in sorted R1441G $Thy1^+/CD3^-$ neurons, $GLAST^+$ astrocytes and $O4^+$ oligodendrocytes following *in vivo* LPS treatment. Relative band intensities of LRRK2 are normalized to β-actin. For each cell population fold change represents LRRK2 expression in LPS-treated group compared to NaCl control. (**K**) $Lrrk2^{-/-}$ brain samples were used to demonstrate anti-LRRK2 antibody specificity.

mononuclear cell subpopulations in mutant LRRK2 mice and wild-type controls, and observed no significant difference in the number of lymphocyte subpopulations, macrophages and granulocytes between the two different genotypes after LPS exposure (Supplementary Fig. 5C). These data suggest that the upregulation in LRRK2 expression observed in LPS-treated mutant leucocytes are due to an increase in the expression of the protein on a per cell basis, and not to a different expansion of the number of mononuclear cells between the two genotypes. Subsequent FACS revealed that $CD19^+$ B-lymphocytes are the main cells contributing to the increase in mutant LRRK2 expression (Fig. 6E). The observation that R1441G mice display a different peripheral cytokine profile in response to LPS next prompted us to determine the molecular pathways that might be affected by mutant LRRK2 in peripheral immune cells. To this end, we performed TMT-based proteomic analysis of the whole proteome of leucocytes isolated from non-treated and LPS-treated R1441G and wild-type mice (Fig. 6A). LRRK2 transgenic leucocytes and wild-type cells showed similar immune-response related protein expression in non-treated condition, however, differed significantly after the stimulation with LPS. Based on gene set enrichment analysis, we identified proteins in the IFN-γ response and inflammatory pathways (Fig. 6F and G) as being significantly enriched in leucocytes isolated from LPS-treated R1441G compared to LPS-treated wild-type mice. The highest overexpressed proteins in LPS-treated R1441G immune cells included antigen processing proteins (FCGR1, H2-Aa, TLR2), transcriptional factors (SP110, IRF8, IRF5, IRF9 and IRF4), mediators of apoptosis (GZMA, CASP1, CASP4, CASP8, PML), cytokines (IL18,

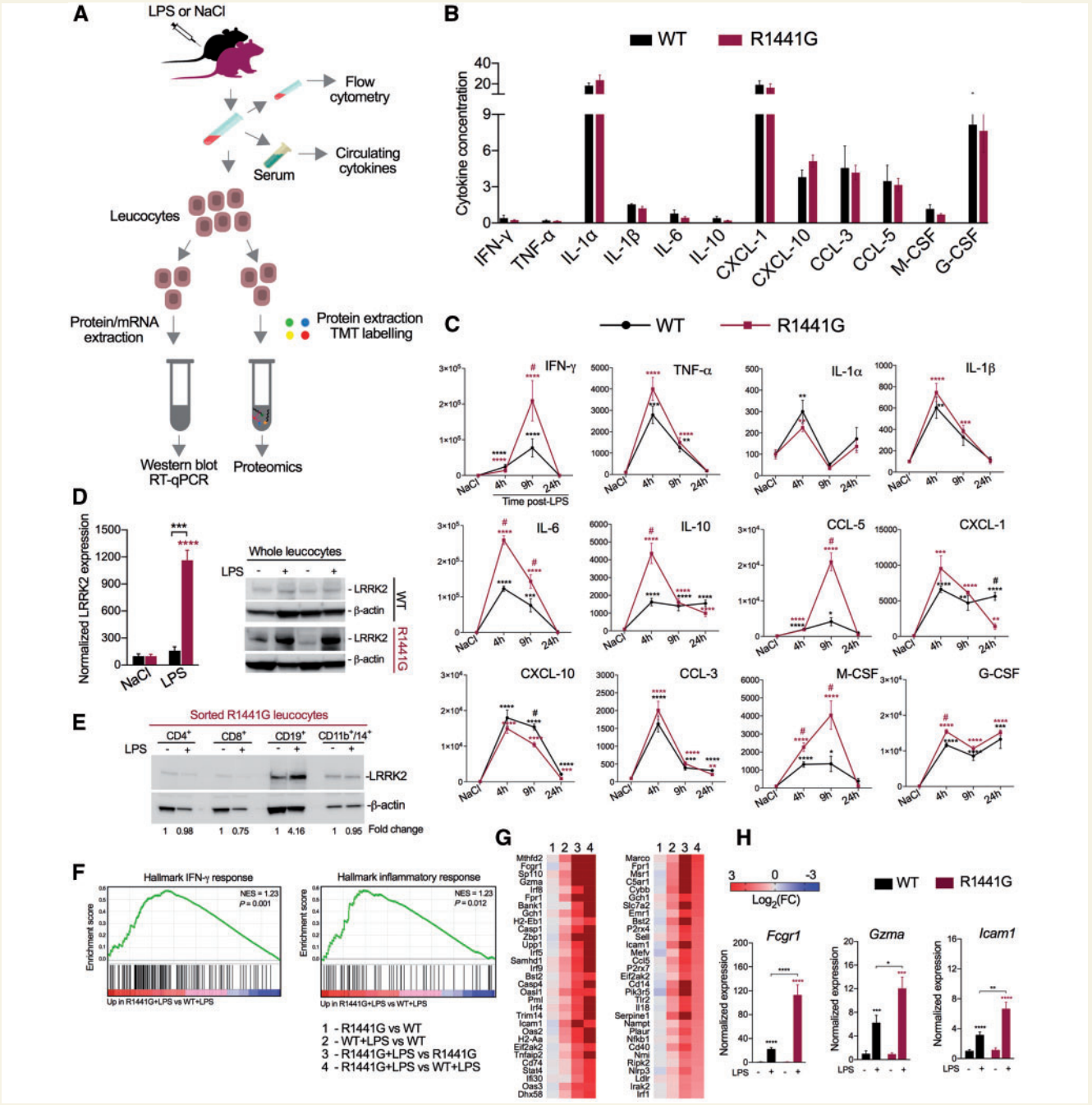

Figure 6 LPS-induced peripheral cytokines secretion and activation of immune pathways in leucocytes are exacerbated by mutant LRRK2. (**A**) Experimental scheme of peripheral immune response analysis. (**B**) Peripheral cytokines profile in the normal R1441G mice and wild-type littermate controls. Data are expressed as pg/mg total protein. Data are mean ± SEM, n = 5–8. (**C**) Inflammatory response in serum of LPS-treated R1441G mice compared to wild-type littermate controls. Data are mean ± SEM, n = 5–8 for NaCl and each post-LPS group. $^{*}P < 0.05$, $^{**}P < 0.01$, $^{***}P < 0.001$, $^{****}P < 0.0001$ versus NaCl group; $^{\#}P < 0.05$ versus LPS-treated wild-type. For each genotype data in LPS-treated groups are expressed as the percentage of NaCl control. (**D**) LRRK2 upregulation in leucocytes following *in vivo* LPS administration. Data are mean ± SEM, n = 4–5 for NaCl and 24 h post-LPS group. $^{***}P < 0.001$, $^{****}P < 0.0001$. (**E**) LRRK2 upregulation in sorted R1441G CD19^{+} B lymphocytes following *in vivo* LPS administration. For all groups, cells were pooled from 15 NaCl- or LPS-treated R1441G mice. (**F**) GSEA plots and (**G**) heat maps showing upregulation of IFN-γ response proteins and Inflammatory response proteins in isolated R1441G leucocytes by comparison with wild-type cells following *in vivo* LPS administration. Each bar at the bottom of panel in **F** represents a member protein of the respective pathway. For each gene set enrichment assay, the nominal P-value and normalized enrichment score (NES) are shown. (**H**) mRNA expression of the selected genes in the leucocytes isolated from NaCl- and LPS-treated R1441G and wild-type littermate mice validated in an independent RT-qPCR experiment. Target genes expression level was normalized to β-actin. Data are mean ± SEM, n = 4–5 for NaCl group; n = 3 for LPS group (for each n, cells were pooled from three mice). $^{*}P < 0.05$, $^{**}P < 0.01$, $^{***}P < 0.001$, $^{****}P < 0.0001$.

CCL5), regulators of NF-κB (ICAM1, CD40, NFKB1, TRIM14) and MAPK signalling (FPR1) (Fig. 6G). Thus, mutant LRRK2 dysregulates LPS-induced activation of immune response related pathways in circulating mononuclear cells during the acute phase of inflammation.

Overall, the data in this study suggest that LPS-induced elevated neuroinflammation and neuronal loss in LRRK2 mutants are most likely initiated through circulating inflammatory mediators rather than a direct T cell or monocyte-mediated (both, microglia and macrophages) neurotoxicity.

Discussion

LRRK2 missense mutations are responsible for both familial and non-familial forms of late-onset Parkinson's disease in humans (Zimprich *et al.*, 2004); however, the precise mechanisms by which LRRK2 induces pathology are still unclear. Low penetrance of the mutations in humans (Bonifati, 2007; Goldwurm *et al.*, 2007; Latourelle *et al.*, 2008; Xiromerisiou *et al.*, 2012), and the absence of an obvious neurological phenotype in LRRK2 mouse models (Tong *et al.*, 2009; Li *et al.*, 2010; Melrose *et al.*, 2010; Herzig *et al.*, 2012; Maekawa *et al.*, 2012; Longo *et al.*, 2014) suggest that Parkinson's disease may result from a complex interplay of genetic predispositions and persistent exogenous insults. Causative factors include pathogens (bacterial or viral infections) (Puccini *et al.*, 2015), protein aggregates (α-synuclein) (Deleidi and Gasser, 2013) or immune alterations associated with ageing or autoimmune disorders (Liu and Lenardo, 2012). In this study, we report new findings that expand our understanding by which LRRK2 mutations contribute to the development of Parkinson's disease: (i) we demonstrate that LPS-induced inflammation is able to synergize with mutant LRRK2 (both R1441G and G2019S) to potentiate SNpc dopaminergic neuronal loss; (ii) we show that neurodegeneration is accompanied by an exacerbated neuroinflammation in the CNS, which has a subsequent effect on neurons by inducing intraneuronal LRRK2 upregulation; (iii) we provide evidence that enhanced neuroinflammation is not triggered by the brain's resident microglia or infiltrated immune cells; and (iv) we show that mutant LRRK2 alters peripheral immune response and provides the first evidence of what inflammation related pathways could be modified by the pathogenic LRRK2 mutation.

One potential caveat to our findings is that these studies were carried out in mice that overexpressed mutant human LRRK2, rather than in mice carrying a knocked-in point mutation in the murine *Lrrk2* gene (Herzig *et al.*, 2011; Yue *et al.*, 2015). We chose to use the human mutant LRRK2 BAC overexpression model for several reasons. First, knock-in G2019S mice develop neither neuronal loss/overt neuropathology nor abnormal locomotor response to dopaminergic agonists/antagonists (Herzig *et al.*, 2011), suggesting that these knock-in LRRK2 mice do not phenocopy the human Parkinson's disease pathology. Second, although the homology between the mouse and human *LRRK2* gene is high [up to 94% in the ROC domain and 97% in the kinase domain (Langston *et al.*, 2016)], it has been noted that there are significant differences in the gene's regulatory regions (West *et al.*, 2014). This lack of homology in the regulatory region could lead to differences in site(s) of protein expression as well as how the protein expresses in response to exogenous factors. For these reasons, we felt that use of the human BAC transgenic mice was an appropriate model for our studies. An additional caveat to our studies is that we cannot exclude the possibility that simply the overexpression of LRRK2 protein may, to some extent, alter the immune response; although have shown that LPS-induced inflammation in WT-OX mice does not result in neuronal loss, i.e. a parkinsonian phenotype. Additionally, recent studies found that WT-OX mice did not show statistically significant differences in peripheral monocyte subset ratios compared to R1441G mice (Bliederhaeuser *et al.*, 2016), and the overexpression of wild-type LRRK2 had no effect on LPS-induced cytokine secretion by macrophages and on myeloid cell chemotaxis compared to non-transgenic cells (Moehle *et al.*, 2015). Therefore, because of the lack of LPS-induced neurodegeneration in WT-OX mice, most experimental data on R1441G and/or G2019S were compared with background- and age-matched wild-type mice.

In this study, we do not observe LPS-induced SNpc dopaminergic neuron loss in wild-type mice; most likely due to the fact that the upregulation of pro-inflammatory mediators in the substantia nigra of wild-type mice is transient, returning to normal levels relatively quickly (within a week); i.e. the brain parenchyma is able to modulate the neuroinflammatory response. However, unlike what was observed in wild-type mice, LRRK2 mutant mice exhibited an exaggerated long-term microglial activation with extended secretion of inflammatory factors, including IFN-γ and IL-1α, that have been shown to mediate dopaminergic neuron degeneration (Pott Godoy *et al.*, 2008; Chakrabarty *et al.*, 2011; Mangano *et al.*, 2012). The finding of enhanced SNpc dopaminergic neuron loss in the R1441G LRRK2 mutant mice subsequent to LPS exposure with continued cytokine/chemokine secretion suggests an ongoing process where inflammatory factors provoke a cycle of inflammation in the brain that eventually reaches a critical 'threshold', triggering a self-perpetuating cycle of inflammation and neurodegeneration. Critically, we showed for the first time that ongoing neuroinflammation leads to the upregulation of intraneuronal mutant LRRK2 *in vivo*, which may also subsequently contribute to neurotoxicity observed in mutant mice since intraneuronal LRRK2 level has been shown to be proportional to cell death (Skibinski *et al.*, 2014).

Since microglia, because of its high expression of TLR4 (Zhou *et al.*, 2006), are the primary cells capable of responding to the inflammatory stimulus in the brain, we hypothesized that neuroinflammation in the CNS of LRRK2 mice, especially in the substantia nigra, which is enriched with microglia (Lawson *et al.*, 1990), could be

directly exacerbated by the mutant microglial LRRK2. However, unlike recent findings showing wild-type LRRK2 upregulation after intranigral injection of LPS in isolectin B4$^+$ cells with a morphology and size consistent with activated microglia (Moehle *et al.*, 2012), we did not detect LRRK2 expression in microglia isolated from either whole brain or midbrain, both before and after LPS-induced inflammation. What could explain this difference? Bearing in mind that peripheral monocytes have detectable expression of LRRK2, and intracerebral, but not peripheral, LPS injection induces a massive extravasation of leucocytes into the brain parenchyma (Zhou *et al.*, 2006; Ji *et al.*, 2007), we postulate that that the LRRK2$^+$/isolectin B4$^+$ cells are not resident microglia, but most likely represent monocytes from the periphery that invade the CNS. This hypothesis is supported by recent studies from the West lab, who showed LRRK2 immunoreactivity in CD68/iNOS-positive cells recruited in response to α-synuclein and LPS-transduced SNpc (Daher *et al.*, 2014).

The lack of LRRK2 expression in microglia has also been shown in numerous immunohistochemical and *in situ* hybridization studies on brain sections obtained from healthy controls and patients with Parkinson's disease. These studies demonstrated that LRRK2 protein and/or mRNA was localized exclusively to neuronal perikarya and dendritic/axonal processes (Higashi *et al.*, 2007; Hakimi *et al.*, 2011; Sharma *et al.*, 2011; Dzamko *et al.*, 2012, 2017). Furthermore, microglia from adult wild-type mice and BAC transgenic LRRK2 mice do not show any LRRK2 immunoreactivity *in vivo* (Biskup *et al.*, 2006; Higashi *et al.*, 2007; Westerlund *et al.*, 2008; Mandemakers *et al.*, 2012). However, we recognize that the finding of a lack of LRRK2 expression in adult microglia is somewhat controversial. Indeed, initial *in vitro* studies examining this showed that a relatively high level of LRRK2 was expressed in mouse peripheral macrophages, monocytes (Gardet *et al.*, 2010) and cultured bone marrow-derived macrophages (Hakimi *et al.*, 2011). These findings led to the uniform assumption that LRRK2 is expressed in all cell types of myeloid origin, at any developmental stage. Others have shown that primary P2 rat microglia (Moehle *et al.*, 2012) and the immortalized murine microglial cell line, BV-2 (Kim *et al.*, 2012; Russo *et al.*, 2015) also express LRRK2. However, this expression was seen in cultured and/or immortalized cells that have been shown to act substantially different from cognate CNS resident microglia (Schmid *et al.*, 2009); including the significant finding that they do not express the molecular signature(s) seen in adult microglial cells (Butovsky *et al.*, 2014).

Our results, in concert with previous studies that demonstrated no microglia-specific LRRK2 protein and/or mRNA expression in the brain sections from healthy controls and patients with Parkinson's disease (Higashi *et al.*, 2007; Hakimi *et al.*, 2011; Sharma *et al.*, 2011; Dzamko *et al.*, 2012, 2017), support the hypothesis that 'mutant' microglia cannot directly alter neuroinflammation in the brain of mice overexpressing the parkinsonian mutation, and for the first time raise an important question of whether LRRK2 mutations impair peripheral immune cell function(s) with a deleterious impact on brain microglia and dopaminergic neurons as a secondary effect.

This leads us to propose that the exacerbated neuroinflammation measured in the CNS of mice carrying LRRK2 mutations occurs as a peripheral-to-centrally-mediated immune signal, and does not depend on the active participation of microglia or infiltrating T cells and monocytes. In fact, by monitoring circulating cytokine production and inflammatory signalling in peripheral leucocytes of LPS-challenged wild-type and mutant LRRK2 mice, we demonstrated that this Parkinson's disease-causing mutation significantly dysregulates LPS-induced activation of peripheral cytokines and inflammatory proteins in the leucocytes, including IFN-inducible proteins (SP110, IRF8, IRF5, IRF9 and IRF4), antigen processing proteins (TLR2, FCGR1, H2-Aa) and crucial mediators of NF-κB and MAPK signalling (ICAM1, CD40, NFKB1, TRIM14, FPR1). Although the mechanisms connecting the peripheral immune response and neuroinflammation are not yet fully understood, it is known that blood-borne cytokines, including IL-1α, IL-1β, IL-6 and TNF-α can reach the brain and transduce the inflammatory response to relevant cell types through either 'leaky' regions in the blood–brain barrier located in the circumventricular organs (passive diffusion) or directly via saturable transport systems on endothelial cells (Banks *et al.*, 1995; Pan *et al.*, 2011). Once activated by blood-borne cytokines, both microglia and endothelial cells expressing cytokine receptors (Van Dam *et al.*, 1996; Reyes *et al.*, 1999; Verma *et al.*, 2006) may subsequently amplify a cascade of local neurotoxic mediators even after resolution of the peripheral inflammation. However, microglia and endothelial cells in LRRK2 mutants seem to not be related to the accelerated neuroinflammatory response *per se*, but act more in a modulatory rather than primary role. Importantly, one should keep in mind that although the blood–brain barrier is almost impermeable to LPS (Nadeau and Rivest, 2002; Banks and Robinson, 2010), TLR4-positive cells were found along large brain vessels and within the choroid plexus, meninges, circumventricular organs, and the ventricular ependymal lining (Chakravarty and Herkenham, 2005). If endothelial cells possess the ability to express LRRK2, they might also alter the cascade of inflammatory signals initiated by peripherally administrated LPS, though unlikely since LRRK2 has been found so far only in human umbilical vein endothelial cells (Hongge *et al.*, 2015), and little is known about its expression in brain microvascular endothelial cells.

Several clinical reports have reported on the association of alterations in the peripheral immune response associated with familial Parkinson's disease to central inflammation and neurodegeneration. For example, the involvement of peripheral inflammation in LRRK2-associated Parkinson's disease can be supported by studies demonstrating dysregulated interleukin and TGF-β signalling in immune cells from G2019S patients (Mutez *et al.*, 2011), as well as the

increase in peripheral pro-inflammatory cytokines in the asymptomatic G2019S carriers (Dzamko *et al.*, 2016). Moreover, a genome-wide association study revealed a possible involvement of different single-nucleotide polymorphisms in the *LRRK2* gene in Crohn's disease, an inflammatory bowel disease (Franke *et al.*, 2010), and leprosy, a chronic infectious disease caused by *Mycobacterium leprae* (Zhang *et al.*, 2009; Fava *et al.*, 2016). The widespread distribution of LRRK2 in peripheral tissues related to immune response and its genetic implication in inflammatory disorders such as Crohn's disease and leprosy reinforce the notion that LRRK2 may act as a regulator of the immune system. Indeed, recent *in vitro* studies have demonstrated a robust IFN-γ-stimulated increase of endogenous wild-type LRRK2 expression across various subsets of cultured myeloid cells, lymphocytes, bone marrow-derived macrophages and transformed cell lines, including human THP-1 cells and murine RAW264.7 macrophage-like cells (Gardet *et al.*, 2010; Hakimi *et al.*, 2011; Gillardon *et al.*, 2012; Kuss *et al.*, 2014). However, our data clearly indicate that under *in vivo* stimulating conditions, mutant LRRK2 is solely upregulated in lymphocytes, an in particular B lymphocytes, and not in myeloid cell lineage (peripheral macrophages or CNS microglia), while wild-type LRRK2 seems to be unchanged in all types of cells. Given that *in vivo* interactions between immune cells are extremely dynamic and appear to be bidirectional, the physiological interactome of mutant LRRK2 in 'authentic' immune cells could be far more complex than those seen *in vitro*. Our observation that B lymphocytes display activated mutant LRRK2 over other immune cells under stimulated conditions along with the studies showing high LRRK2 expression in human B cells (Gardet *et al.*, 2010; Hakimi *et al.*, 2011; Thevenet *et al.*, 2011) raises the intriguing question of whether B cell-derived LRRK2 could be involved in the regulation of immune response to pathogens through secreted antibodies or by cellular interactions and/or cytokine-dependent mechanisms. Therefore, future in-depth examinations of immune response and LRRK2 activation in B cells derived from idiopathic and LRRK2 Parkinson's disease patients may help clarify the role of mutant LRRK2 in health and disease. In addition, further *in vivo* studies on transgenic mice lacking mutant LRRK2 expression in lymphocyte subsets with mutant LRRK2 expression in the nervous system are required to define the mechanism(s) connecting the peripheral immune response with neurodegeneration in the CNS.

Acknowledgements

We thank Drs Ben Barres and Mariko Bennett (Stanford University School of Medicine) for providing Tmem119 antibody; Dr Mark Cookson (Laboratory of Neurogenetics, National Institute of Aging, NIH) for providing *Lrrk2*$^{-/-}$ samples; Drs Mark Valentine and Virginia Valentine from the St. Jude Cytogenetic Core for performing FISH analysis; Drs Richard Ashmun and Stacie Woolard from St. Jude Flow Cytometry and Cell Sorting Shared Resource for assistance with Flow Cytometry and Cell Sorting; Dr Jamshid Temirov from St Jude Cell and Tissue Imaging Center for assistance with light microscopy and imaging.

Funding

Supported by Cancer Center Support Grant P30 CA021765, The American-Lebanese Syrian Associated Charity and Thomas Jefferson University.

Supplementary material

Supplementary material is available at *Brain* online.

References

Allan SM, Rothwell NJ. Cytokines and acute neurodegeneration. Nat Rev Neurosci 2001; 2: 734–44.

Allan SM, Tyrrell PJ, Rothwell NJ. Interleukin-1 and neuronal injury. Nat Rev Immunol 2005; 5: 629–40.

Banks WA, Kastin A, Broadwell RD. Passage of cytokines across the blood-brain barrier. Neuroimmunomodulation 1995; 2: 241–8.

Banks WA, Robinson SM. Minimal penetration of lipopolysaccharide across the murine blood-brain barrier. Brain Behav Immun 2010; 24: 102–9.

Baquet ZC, Williams D, Brody J, Smeyne RJ. A comparison of model-based (2D) and design-based (3D) stereological methods for estimating cell number in the substantia nigra pars compacta (SNpc) of the C57BL/6J mouse. Neuroscience 2009; 161: 1082–90.

Bekris LM, Mata IF, Zabetian CP. The genetics of Parkinson disease. J Geriatr Psychiatry Neurol 2010; 23: 228–42.

Bennett ML, Bennett FC, Liddelow SA, Ajami B, Zamanian JL, Fernhoff NB, et al. New tools for studying microglia in the mouse and human CNS. Proc Natl Acad Sci USA 2016; 113: E1738–46.

Bichler Z, Lim HC, Zeng L, Tan EK. Non-motor and motor features in LRRK2 transgenic mice. PLoS One 2013; 8: e70249.

Biskup S, Moore DJ, Celsi F, Higashi S, West AB, Andrabi SA, et al. Localization of LRRK2 to membranous and vesicular structures in mammalian brain. Ann Neurol 2006; 60: 557–69.

Bliederhaeuser C, Zondler L, Grozdanov V, Ruf WP, Brenner D, Melrose HL, et al. LRRK2 contributes to monocyte dysregulation in Parkinson's disease. Acta Neuropathol Commun 2016; 4: 123.

Bonifati V. LRRK2 low-penetrance mutations (Gly2019Ser) and risk alleles (Gly2385Arg)-linking familial and sporadic Parkinson's disease. Neurochem Res 2007; 32: 1700–8.

Brewer GJ, Torricelli JR. Isolation and culture of adult neurons and neurospheres. Nat Protoc 2007; 2: 1490–8.

Brochard V, Combadiere B, Prigent A, Laouar Y, Perrin A, Beray-Berthat V, et al. Infiltration of CD4+ lymphocytes into the brain contributes to neurodegeneration in a mouse model of Parkinson disease. J Clin Invest 2009; 119: 182–92.

Brodacki B, Staszewski J, Toczylowska B, Kozlowska E, Drela N, Chalimoniuk M, et al. Serum interleukin (IL-2, IL-10, IL-6, IL-4), TNFalpha, and INFgamma concentrations are elevated in patients with atypical and idiopathic parkinsonism. Neurosci Lett 2008; 441: 158–62.

Butovsky O, Jedrychowski MP, Moore CS, Cialic R, Lanser AJ, Gabriely G, et al. Identification of a unique TGF-beta-dependent

molecular and functional signature in microglia. Nat Neurosci 2014; 17: 131–43.
Cardona AE, Huang D, Sasse ME, Ransohoff RM. Isolation of murine microglial cells for RNA analysis or flow cytometry. Nat Protoc 2006; 1: 1947–51.
Cebrian C, Zucca FA, Mauri P, Steinbeck JA, Studer L, Scherzer CR, et al. MHC-I expression renders catecholaminergic neurons susceptible to T-cell-mediated degeneration. Nat Commun 2014; 5: 3633.
Chakrabarty P, Ceballos-Diaz C, Lin WL, Beccard A, Jansen-West K, McFarland NR, et al. Interferon-gamma induces progressive nigrostriatal degeneration and basal ganglia calcification. Nat Neurosci 2011; 14: 694–6.
Chakravarty S, Herkenham M. Toll-like receptor 4 on nonhematopoietic cells sustains CNS inflammation during endotoxemia, independent of systemic cytokines. J Neurosci 2005; 25: 1788–96.
Chiu IM, Morimoto ET, Goodarzi H, Liao JT, O'Keeffe S, Phatnani HP, et al. A neurodegeneration-specific gene-expression signature of acutely isolated microglia from an amyotrophic lateral sclerosis mouse model. Cell Rep 2013; 4: 385–401.
Daher JP, Volpicelli-Daley LA, Blackburn J, Moehle MS, West AB. Abrogation of α-synuclein–mediated dopaminergic neurodegeneration in LRRK2-deficient rats. Proc Natl Acad Sci USA 2014; 111: 9289–94.
Deleidi M, Gasser T. The role of inflammation in sporadic and familial Parkinson's disease. Cell Mol Life Sci 2013; 70: 4259–73.
Dufek M, Hamanova M, Lokaj J, Goldemund D, Rektorova I, Michalkova Z, et al. Serum inflammatory biomarkers in Parkinson's disease. Parkinsonism Relat Disord 2009; 15: 318–20.
Dzamko N, Gysbers AM, Bandopadhyay R, Bolliger MF, Uchino A, Zhao Y, et al. LRRK2 levels and phosphorylation in Parkinson's disease brain and cases with restricted Lewy bodies. Mov Disord 2017; 32: 423–32.
Dzamko N, Inesta-Vaquera F, Zhang J, Xie C, Cai H, Arthur S, et al. The IkappaB kinase family phosphorylates the Parkinson's disease kinase LRRK2 at Ser935 and Ser910 during Toll-like receptor signaling. PLoS One 2012; 7: e39132.
Dzamko N, Rowe DB, Halliday GM. Increased peripheral inflammation in asymptomatic leucine-rich repeat kinase 2 mutation carriers. Mov Disord 2016; 31: 889–97.
Fava VM, Manry J, Cobat A, Orlova M, Van Thuc N, Ba NN, et al. A Missense LRRK2 variant is a risk factor for excessive inflammatory responses in leprosy. PLoS Negl Trop Dis 2016; 10: e0004412.
Frank MG, Wieseler-Frank JL, Watkins LR, Maier SF. Rapid isolation of highly enriched and quiescent microglia from adult rat hippocampus: immunophenotypic and functional characteristics. J Neurosci Methods 2006; 151: 121–30.
Franke A, McGovern DP, Barrett JC, Wang K, Radford-Smith GL, Ahmad T, et al. Genome-wide meta-analysis increases to 71 the number of confirmed Crohn's disease susceptibility loci. Nat Genet 2010; 42: 1118–25.
Funayama M, Hasegawa K, Ohta E, Kawashima N, Komiyama M, Kowa H, et al. An LRRK2 mutation as a cause for the parkinsonism in the original PARK8 family. Ann Neurol 2005; 57: 918–21.
Funayama M, Li Y, Tomiyama H, Yoshino H, Imamichi Y, Yamamoto M, et al. Leucine-Rich Repeat kinase 2 G2385R variant is a risk factor for Parkinson disease in Asian population. Mol Neurosci 2006; 18: 273–5.
Gaig C, Ezquerra M, Marti MJ, Muñoz E, Valldeoriola F, Tolosa E. LRRK2 mutations in Spanish patients with Parkinson disease. Arch Neurol 2006; 63: 377–82.
Gardet A, Benita Y, Li C, Sands BE, Ballester I, Stevens C, et al. LRRK2 is involved in the IFN-gamma response and host response to pathogens. J Immunol 2010; 185: 5577–85.
Gillardon F, Schmid R, Draheim H. Parkinson's disease-linked leucine-rich repeat kinase 2(R1441G) mutation increases proinflammatory cytokine release from activated primary microglial cells and resultant neurotoxicity. Neuroscience 2012; 208: 41–8.
Goldwurm S, Zini M, Mariani L, Tesei S, Miceli R, Sironi F, et al. Evaluation of LRRK2 G2019S penetrance: relevance for genetic counseling in Parkinson disease. Neurology 2007; 68: 1141–3.
Gorostidi A, Ruiz-Martinez J, Lopez de Munain A, Alzualde A, Marti Masso JF. LRRK2 G2019S and R1441G mutations associated with Parkinson's disease are common in the Basque Country, but relative prevalence is determined by ethnicity. Neurogenetics 2009; 10: 157–9.
Greggio E, Jain S, Kingsbury A, Bandopadhyay R, Lewis P, Kaganovich A, et al. Kinase activity is required for the toxic effects of mutant LRRK2/dardarin. Neurobiol Dis 2006; 23: 329–41.
Guez-Barber D, Fanous S, Harvey BK, Zhang Y, Lehrmann E, Becker KG, et al. FACS purification of immunolabeled cell types from adult rat brain. J Neurosci Methods 2012; 203: 10–18.
Hakimi M, Selvanantham T, Swinton E, Padmore RF, Tong Y, Kabbach G, et al. Parkinson's disease-linked LRRK2 is expressed in circulating and tissue immune cells and upregulated following recognition of microbial structures. J Neural Transm 2011; 118: 795–808.
Haugarvoll K, Rademakers R, Kachergus JM, Nuytemans K, Ross OA, Gibson JM, et al. Lrrk2 R1441C parkinsonism is clinically similar to sporadic Parkinson disease. Neurology 2008; 70 (16 Pt 2): 1456–60.
Haugarvoll K, Wszolek ZK. Clinical features of LRRK2 parkinsonism. Parkinsonism Relat Disord 2009; 15 (Suppl 3): S205–8.
Healy DG, Falchi M, O'Sullivan SS, Bonifati V, Durr A, Bressman S, et al. Phenotype, genotype, and worldwide genetic penetrance of LRRK2-associated Parkinson's disease: a case-control study. Lancet Neurol 2008; 7: 583–90.
Herzig MC, Bidinosti M, Schweizer T, Hafner T, Stemmelen C, Weiss A, et al. High LRRK2 levels fail to induce or exacerbate neuronal alpha-synucleinopathy in mouse brain. PLoS One 2012; 7: e36581.
Herzig MC, Kolly C, Persohn E, Theil D, Schweizer T, Hafner T, et al. LRRK2 protein levels are determined by kinase function and are crucial for kidney and lung homeostasis in mice. Hum Mol Genet 2011; 20: 4209–23.
Higashi S, Moore DJ, Colebrooke RE, Biskup S, Dawson VL, Arai H, et al. Expression and localization of Parkinson's disease-associated leucine-rich repeat kinase 2 in the mouse brain. J Neurochem 2007; 100: 368–81.
Hofmann KW, Schuh AF, Saute J, Townsend R, Fricke D, Leke R, et al. Interleukin-6 serum levels in patients with Parkinson's disease. Neurochem Res 2009; 34: 1401–4.
Hongge L, Kexin G, Xiaojie M, Nian X, Jinsha H. The role of LRRK2 in the regulation of monocyte adhesion to endothelial cells. J Mol Neurosci 2015; 55: 233–9.
Jaleel M, Nichols RJ, Deak M, Campbell DG, Gillardon F, Knebel A, et al. LRRK2 phosphorylates moesin at threonine-558: characterization of how Parkinson's disease mutants affect kinase activity. Biochem J 2007; 405: 307–17.
Jang H, Boltz D, Sturm-Ramirez K, Shepherd KR, Jiao Y, Webster R et al. Highly pathogenic H5N1 influenza virus can enter the central nervous system and induce neuroinflammation and neurodegeneration. Proc Natl Acad Sci USA 2009; 106: 14063–8.
Ji KA, Yang MS, Jeong HK, Min KJ, Kang SH, Jou I, et al. Resident microglia die and infiltrated neutrophils and monocytes become major inflammatory cells in lipopolysaccharide-injected brain. Glia 2007; 55: 1577–88.
Khan NL, Jain S, Lynch JM, Pavese N, Abou-Sleiman P, Holton JL, et al. Mutations in the gene LRRK2 encoding dardarin (PARK8) cause familial Parkinson's disease: clinical, pathological, olfactory and functional imaging and genetic data. Brain 2005; 128 (Pt 12): 2786–96.
Kim B, Yang MS, Choi D, Kim JH, Kim HS, Seol W, et al. Impaired inflammatory responses in murine Lrrk2-knockdown brain microglia. PLoS One 2012; 7: e34693.
Kumari U, Tan EK. LRRK2 in Parkinson's disease: genetic and clinical studies from patients. FEBS J 2009; 276: 6455–63.

Kuss M, Adamopoulou E, Kahle PJ. Interferon-gamma induces leucine-rich repeat kinase LRRK2 via extracellular signal-regulated kinase ERK5 in macrophages. J Neurochem 2014; 129: 980–7.
Langston RG, Rudenko IN, Cookson MR. The function of orthologues of the human Parkinson's disease gene LRRK2 across species: implications for disease modelling in preclinical research. Biochem J 2016; 473: 221–32.
Latourelle JC, Sun M, Lew MF, Suchowersky O, Klein C, Golbe LI, et al. The Gly2019Ser mutation in LRRK2 is not fully penetrant in familial Parkinson's disease: the GenePD study. BMC Med 2008; 6: 32.
Lawson LJ, Perry VH, Dri P, Gordon S. Heterogeneity in the distribution and morphology of microcroglia in the normal adult mouse brain. Neuroscience 1990; 39: 151–70.
Lee BD, Shin JH, VanKampen J, Petrucelli L, West AB, Ko HS, et al. Inhibitors of leucine-rich repeat kinase-2 protect against models of Parkinson's disease. Nat Med 2010; 16: 998–1000.
Lee JK, Tansey MG. Microglia isolation from adult mouse brain. Methods Mol Biol 2013; 1041: 17–23.
Lee JW, Cannon JR. LRRK2 mutations and neurotoxicant susceptibility. Exp Biol Med 2015; 240: 752–9.
Lesage S, Dürr A, Tazir M, Lohmann E, Leutenegger AL, Janin S, et al. LRRK2 G2019S as a cause of Parkinson's disease in North African Arabs. N Engl J Med 2006; 354: 422–3.
Lewis PA, Manzoni C. LRRK2 and human disease: a complicated question or a question of complexes? Sci Signal 2012; 5: pe2.
Li X, Patel JC, Wang J, Avshalumov MV, Nicholson C, Buxbaum JD, et al. Enhanced striatal dopamine transmission and motor performance with LRRK2 overexpression in mice is eliminated by familial Parkinson's disease mutation G2019S. J Neurosci 2010; 30: 1788–97.
Li Y, Liu W, Oo TF, Wang L, Tang Y, Jackson-Lewis V, et al. Mutant LRRK2(R1441G) BAC transgenic mice recapitulate cardinal features of Parkinson's disease. Nat Neurosci 2009; 12: 826–8.
Liu Z, Lenardo MJ. The role of LRRK2 in inflammatory bowel disease. Cell Res 2012; 22: 1092–4.
Longo F, Russo I, Shimshek DR, Greggio E, Morari M. Genetic and pharmacological evidence that G2019S LRRK2 confers a hyperkinetic phenotype, resistant to motor decline associated with aging. Neurobiol Dis 2014; 71: 62–73.
Lu CS, Simons EJ, Wu-Chou YH, Fonzo AD, Chang HC, Chen RS, et al. The LRRK2 I2012T, G2019S, and I2020T mutations are rare in Taiwanese patients with sporadic Parkinson's disease. Parkinsonism Relat Disord 2005; 11: 521–2.
Luzon-Toro B, Rubio de la Torre E, Delgado A, Perez-Tur J, Hilfiker S. Mechanistic insight into the dominant mode of the Parkinson's disease-associated G2019S LRRK2 mutation. Hum Mol Genet 2007; 16: 2031–9.
Maekawa T, Mori S, Sasaki Y, Miyajima Y, Azuma S, Ohta E, et al. The I2020T Leucine-rich repeat kinase 2 transgenic mouse exhibits impaired locomotive ability accompanied by dopaminergic neuron abnormalities. Mol Neurodegener 2012; 7: 15.
Mandemakers W, Snellinx A, O'Neill MJ, de Strooper B. LRRK2 expression is enriched in the striosomal compartment of mouse striatum. Neurobiol Dis 2012; 48: 582–93.
Mangano E, Litteljohn D, So R, Nelson E, Peters S, Bethune C, et al. Interferon- plays a role in paraquat-induced neurodegeneration involving oxidative and proinflammatory pathways. Neurobiol Aging 2012; 33: 1411–26.
McGeer PL, Itagaki S, McGeer EG. Expression of the histocompatibility glycoprotein HLA-DR in neurological disease. Acta Neuropathol 1988; 76: 550–7.
Melrose HL, Dachsel JC, Behrouz B, Lincoln SJ, Yue M, Hinkle KM, et al. Impaired dopaminergic neurotransmission and microtubule-associated protein tau alterations in human LRRK2 transgenic mice. Neurobiol Dis 2010; 40: 503–17.
Mikhail F, Calingasan N, Parolari L, Subramanian A, Yang L, Flint Beal M. Lack of exacerbation of neurodegeneration in a double transgenic mouse model of mutant LRRK2 and tau. Hum Mol Genet 2015; 24: 3545–56.
Mildner A, Schmidt H, Nitsche M, Merkler D, Hanisch UK, Mack M, et al. Microglia in the adult brain arise from Ly-6ChiCCR2 + monocytes only under defined host conditions. Nat Neurosci 2007; 10: 1544–53.
Mizuno T, Zhang G, Takeuchi H, Kawanokuchi J, Wang J, Sonobe Y, et al. Interferon-gamma directly induces neurotoxicity through a neuron specific, calcium-permeable complex of IFN-gamma receptor and AMPA GluR1 receptor. FASEB J 2008; 22: 1797–806.
Mizutani M, Pino PA, Saederup N, Charo IF, Ransohoff RM, Cardona AE. The fractalkine receptor but not CCR2 is present on microglia from embryonic development throughout adulthood. J Immunol 2012; 188: 29–36.
Moehle MS, Daher JP, Hull TD, Boddu R, Abdelmotilib HA, Mobley J, et al. The G2019S LRRK2 mutation increases myeloid cell chemotactic responses and enhances LRRK2 binding to actin-regulatory proteins. Hum Mol Genet 2015; 24: 4250–67.
Moehle MS, Webber PJ, Tse T, Sukar N, Standaert DG, DeSilva TM, et al. LRRK2 inhibition attenuates microglial inflammatory responses. J Neurosci 2012; 32: 1602–11.
Moussaud S, Draheim HJ. A new method to isolate microglia from adult mice and culture them for an extended period of time. J Neurosci Methods 2010; 187: 243–53.
Mutez E, Larvor L, Lepretre F, Mouroux V, Hamalek D, Kerckaert JP, et al. Transcriptional profile of Parkinson blood mononuclear cells with LRRK2 mutation. Neurobiol Aging 2011; 32: 1839–48.
Nadeau S, Rivest S. Endotoxemia prevents the cerebral inflammatory wave induced by intraparenchymal lipopolysaccharide injection: role of glucocorticoids and CD14. J Immunol 2002; 169: 3370–81.
Nesic O, Xu GY, McAdoo D, High KW, Hulsebosch C, Perez-Pol R. IL-1 Receptor antagonist prevents apoptosis and caspase-3 activation after spinal cord injury. J Neurotrauma 2001; 18: 947–56.
Nichols RJ, Dzamko N, Morrice NA, Campbell DG, Deak M, Ordureau A, et al. 14-3-3 binding to LRRK2 is disrupted by multiple Parkinson's disease-associated mutations and regulates cytoplasmic localization. Biochem J 2010; 430: 393–404.
Ozelius LJ, Senthil G, Saunders-Pullman R, Ohmann E, Deligtisch A, Tagliati M, et al. LRRK2 G2019S as a cause of Parkinson's disease in Ashkenazi Jews. N Engl J Med 2006; 354: 424–5.
Pan W, Stone K, Hauchou H, Manda V, Zhang Y, Kastin A. Cytokine signaling modulates blood-brain barrier function. Curr Pharm Des 2011; 17: 3729–40.
Paul L, Fraifeld V, Kaplanski J. Evidence supporting involvement of leukotrienes in LPS-induced hypothermia in mice. Am J Physiol 1999; 276: R52–8.
Paxinos G, Franklin KBJ. The mouse brain in stereotaxic coordinates. Vol. 2. San Diego: Academic Press; 2001.
Pott Godoy MC, Tarelli R, Ferrari CC, Sarchi MI, Pitossi FJ. Central and systemic IL-1 exacerbates neurodegeneration and motor symptoms in a model of Parkinson's disease. Brain 2008; 131 (Pt 7): 1880–94.
Puccini JM, Marker DF, Fitzgerald T, Barbieri J, Kim CS, Miller-Rhodes P, et al. Leucine-rich repeat kinase 2 modulates neuroinflammation and neurotoxicity in models of human immunodeficiency virus 1-associated neurocognitive disorders. J Neurosci 2015; 35: 5271–83.
Puschmann A, Englund E, Ross OA, Vilarino-Guell C, Lincoln SJ, Kachergus JM, et al. First neuropathological description of a patient with Parkinson's disease and LRRK2 p.N1437H mutation. Parkinsonism Relat Disord 2012; 18: 332–8.
Ramonet D, Daher JP, Lin BM, Stafa K, Kim J, Banerjee R, et al. Dopaminergic neuronal loss, reduced neurite complexity and autophagic abnormalities in transgenic mice expressing G2019S mutant LRRK2. PLoS One 2011; 6: e18568.
Rentzos M, Nikolaou C, Andreadou E, Paraskevas GP, Rombos A, Zoga M, et al. Circulating interleukin-15 and RANTES chemokine in Parkinson's disease. Acta Neurol Scand 2007; 116: 374–9.

Reyes T, Fabry Z, Coe C. Brain endothelial cell production of a neuroprotective cytokine, interleukin-6, in response to noxious stimuli. Brain Res 1999; 851: 215–20.

Romanovsky AA, Shido O, Sakurada S, Sugimoto N, Nagasaka T. Endotoxin shock-associated hypothermia. Ann N Y Acad Sci 1997; 813: 733–7.

Ross OA, Soto-Ortolaza AI, Heckman MG, Aasly JO, Abahuni N, Annesi G, et al. Association of LRRK2 exonic variants with susceptibility to Parkinson's disease: a case–control study. Lancet Neurol 2011; 10: 898–908.

Russo I, Berti G, Plotegher N, Bernardo G, Filograna R, Bubacco L, et al. Leucine-rich repeat kinase 2 positively regulates inflammation and down-regulates NF-kappaB p50 signaling in cultured microglia cells. J Neuroinflammation 2015; 12: 230.

Sanchez G, Varaschin RK, Bueler H, Marcogliese PC, Park DS, Trudeau LE. Unaltered striatal dopamine release levels in young Parkin knockout, Pink1 knockout, DJ-1 knockout and LRRK2 R1441G transgenic mice. PLoS One 2014; 9: e94826.

Satake W, Nakabayashi Y, Mizuta I, Hirota Y, Ito C, Kubo M, et al. Genome-wide association study identifies common variants at four loci as genetic risk factors for Parkinson's disease. Nat Genet 2009; 41: 1303–7.

Schmid CD, Melchior B, Masek K, Puntambekar SS, Danielson PE, Lo DD, et al. Differential gene expression in LPS/IFNgamma activated microglia and macrophages: in vitro versus in vivo. J Neurochem 2009; 109 (Suppl 1): 117–25.

Schwarz JM, Smith SH, Bilbo SD. FACS analysis of neuronal-glial interactions in the nucleus accumbens following morphine administration. Psychopharmacology 2013; 230: 525–35.

Sharma K, Schmitt S, Bergner CG, Tyanova S, Kannaiyan N, Manrique-Hoyos N, et al. Cell type- and brain region-resolved mouse brain proteome. Nat Neurosci 2015; 18: 1819–31.

Sharma S, Bandopadhyay R, Lashley T, Renton AE, Kingsbury AE, Kumaran R, et al. LRRK2 expression in idiopathic and G2019S positive Parkinson's disease subjects: a morphological and quantitative study. Neuropathol Appl Neurobiol 2011; 37: 777–90.

Sheng Z, Zhang S, Bustos D, Kleinheinz T, Le Pichon CE, Dominguez SL, et al. Ser1292 autophosphorylation is an indicator of LRRK2 kinase activity and contributes to the cellular effects of PD mutations. Sci Transl Med 2012; 4: 164ra161.

Skibinski G, Nakamura K, Cookson MR, Finkbeiner S. Mutant LRRK2 toxicity in neurons depends on LRRK2 levels and synuclein but not kinase activity or inclusion bodies. J Neurosci 2014; 34: 418–33.

Smith WW, Pei Z, Jiang H, Dawson VL, Dawson TM, Ross CA. Kinase activity of mutant LRRK2 mediates neuronal toxicity. Nat Neurosci 2006; 9: 1231–3.

Steger M, Tonelli F, Ito G, Davies P, Trost M, Vetter M, et al. Phosphoproteomics reveals that Parkinson's disease kinase LRRK2 regulates a subset of Rab GTPases. Elife 2016; 5: e12813.

Tan H, Yang K, Li Y, Shaw TI, Wang Y, Blanco DB, et al. Integrative proteomics and phosphoproteomics profiling reveals dynamic signaling networks and bioenergetics pathways underlying T cell activation. Immunity 2017; 46: 488–503.

Thevenet J, Pescini Gobert R, Hooft van Huijsduijnen R, Wiessner C, Sagot YJ. Regulation of LRRK2 expression points to a functional role in human monocyte maturation. PLoS One 2011; 6: e21519.

Tong Y, Pisani A, Martella G, Karouani M, Yamaguchi H, Pothos EN, et al. R1441C mutation in LRRK2 impairs dopaminergic neurotransmission in mice. Proc Natl Acad Sci USA 2009; 106: 14622–7.

Van Dam AM, de Vries HE, Kuiper J, Zijlstra FJ, De Boer AG, Tilders FJ, et al. Interleukin-1 receptors on rat brain endothelial cells: a role in neuroimmune interaction? FASEB J 1996; 10: 351–6.

Verma S, Nakaoke R, Dohgu S, Banks WA. Release of cytokines by brain endothelial cells: a polarized response to lipopolysaccharide. Brain Behav Immun 2006; 20: 449–55.

West AB, Cowell RM, Daher JP, Moehle MS, Hinkle KM, Melrose HL, et al. Differential LRRK2 expression in the cortex, striatum, and substantia nigra in transgenic and nontransgenic rodents. J Comp Neurol 2014; 522: 2465–80.

West AB, Moore D, Biskup S, Bugayenko A, Smith WW, Ross CA, et al. Parkinson's disease-associated mutations in leucine-rich repeat kinase 2 augment kinase activity. Proc Natl Acad Sci USA 2005; 102: 16842–7.

West AB, Moore DJ, Choi C, Andrabi SA, Li X, Dikeman D, et al. Parkinson's disease-associated mutations in LRRK2 link enhanced GTP-binding and kinase activities to neuronal toxicity. Hum Mol Genet 2007; 16: 223–32.

Westerlund M, Belin AC, Anvret A, Bickford P, Olson L, Galter D. Developmental regulation of leucine-rich repeat kinase 1 and 2 expression in the brain and other rodent and human organs: implications for Parkinson's disease. Neuroscience 2008; 152: 429–36.

Wider C, Dickson DW, Wszolek ZK. Leucine-rich repeat kinase 2 gene-associated disease: redefining genotype-phenotype correlation. Neurodegener Dis 2010; 7: 175–9.

Xiromerisiou G, Houlden H, Sailer A, Silveira-Moriyama L, Hardy J, Lees AJ. Identical twins with Leucine rich repeat kinase type 2 mutations discordant for Parkinson's disease. Mov Disord 2012; 27: 1323.

Yue M, Hinkle KM, Davies P, Trushina E, Fiesel FC, Christenson TA, et al. Progressive dopaminergic alterations and mitochondrial abnormalities in LRRK2 G2019S knock-in mice. Neurobiol Dis 2015; 78: 172–95.

Zhang F, Huang W, Chen S, Sun L, Liu H, Li Y, et al. Genome wide association study of leprosy. N Engl J Med 2009; 361: 2609–18.

Zhou H, Lapointe BM, Clark SR, Zbytnuik L, Kubes P. A requirement for microglial TLR4 in leukocyte recruitment into brain in response to lipopolysaccharide. J Immunol 2006; 177: 8103–10.

Zimprich A, Biskup S, Leitner P, Lichtner P, Farrer M, Lincoln S, et al. Mutations in LRRK2 cause autosomal-dominant parkinsonism with pleomorphic pathology. Neuron 2004; 44: 601–7.